Acta Mathematicae Applicatae Sinica, English Series
Vol. 18, No. 1 (2002) 37–62

Acta Mathematicae Applicatae
Sinica, English Series

A Relaxation Scheme for Solving the Boltzmann Equation Based on the Chapman-Enskog Expansion

Shi Jin[1], **Lorenzo Pareschi**[2], **Marshall Slemrod**[3]

[1]Department of Mathematics, University of Wisconsin, Madison, Van Vleck Hall, WI 53706, USA.
(E-mail: jin@math.wisc.edu)
[2]Department of Mathematics, University of Ferrara, Via Machiavelli 35, I-44100, Italy & Department of Mathematics, University of Wisconsin-Madison, Van Vleck Hall, WI 53706, USA. (E-mail: pareschi@dm.unife.it)
[3]Department of Mathematics, University of Wisconsin-Madison, Madison, WI 53715-1149, USA.
(Email: slemrod@math.wisc.edu)

Abstract In [16] a visco-elastic relaxation system, called the relaxed Burnett system, was proposed by Jin and Slemrod as a moment approximation to the Boltzmann equation. The relaxed Burnett system is weakly parabolic, has a linearly hyperbolic convection part, and is endowed with a generalized entropy inequality. It agrees with the solution of the Boltzmann equation up to the Burnett order via the Chapman-Enskog expansion.

We develop a one-dimensional non-oscillatory numerical scheme based on the relaxed Burnett system for the Boltzmann equation. We compare numerical results for stationary shocks based on this relaxation scheme, and those obtained by the DSMC (Direct Simulation Monte Carlo), by the Navier-Stokes equations and by the extended thermodynamics with thirteen moments (the Grad equations). Our numerical experiments show that the relaxed Burnett gives more accurate approximations to the shock profiles of the Boltzmann equation obtained by the DSMC, for a range of Mach numbers for hypersonic flows, than those obtained by the other hydrodynamic systems.

Keywords Boltzmann equation, Chapman-Enskog expansion, Burnett equations, relaxation, central schemes
2000 MR Subject Classification 35L99, 65M06, 76P05, 82C40

1 Introduction

Dynamics of a moderately rarefied gas of monatomic molecules is often represented by the Boltzmann equation. Observable quantities such as density, velocity, temperature, etc., are derived as expectations of a probability density function $f(\boldsymbol{x},\boldsymbol{\xi},t)$ satisfying the Boltzmann equation (see [7, 36])

$$f_+\boldsymbol{\xi}\cdot\nabla f=\frac{1}{\varepsilon}Q(f,f),$$

where $\boldsymbol{x}$ denotes the position of a particle at time t moving with velocity $\boldsymbol{\xi}$, Q is the integral collision operator, and ϵ is the Knudsen number which is proportional to the mean free path of the gas. The main numerical difficulty to solve the Boltzmann equation is its high dimensionality. There are two practical methods being used in applications. One is the DSMC (Direct Simulation Monte-Carlo[3, 30] and the others are moment methods that provide continuum equations for the observable macroscopic equations. DSMC offers much less computational cost than a

Manuscript received October 8, 2001.
[1]Supported by NSF grant DMS-0196106; [3]Supported by NSF grant DMS-9803223 and DMS-00711463.

deterministic method, but on the other hand it yields low accuracy and statistically fluctuating results and the convergence in general is very slow. Moment methods, among them the Grad's thirteen moment equations[13] and the extended Thermodynamics equations[26], defined in physical space, are generally faster than DSMC but the results deviate from that of the Boltzmann at high Mach numbers.

In this paper we propose a new numerical scheme based on the Chapman-Enskog expansion (see [7, 10, 36]) for the Boltzmann equation. This scheme is a numerical discretization of the relaxation approximation proposed by Jin and Slemrod[16, 17] and its conceptual basis is indeed the Chapman-Enskog expansion.

The classical Chapman-Enskog procedure for the Boltzmann equation is a well known tool for bridging the gap between kinetic theory as described by the Boltzmann equation for the evolution of a monatomic gas and continuum mechanics. The Chapman-Enskog expansion is a formal power series ordered by the viscosity μ which is itself proportional to the non-dimensional Knudsen number, i.e.,

$$\begin{aligned} \boldsymbol{T} &= -p\boldsymbol{I} - \boldsymbol{P}, & p &= R\rho\theta, \\ \boldsymbol{P} &= \mu\boldsymbol{\Pi}^{(1)} + \mu^2\boldsymbol{\Pi}^{(2)} + \mu^3\boldsymbol{\Pi}^{(3)} + \cdots, & \boldsymbol{q} &= \mu\boldsymbol{\Xi}^{(1)} + \mu^2\boldsymbol{\Xi}^{(2)} + \mu^3\boldsymbol{\Xi}^{(3)} + \cdots. \end{aligned}$$

The coefficients $\boldsymbol{\Pi}^{(j)}$, $\boldsymbol{\Xi}^{(j)}$, $j = 1, 2, \cdots$ are obtained from the Boltzmann equation and have been determined up to $j = 2$ (Burnett order) (cf. [10, 36]) and in one space dimension up to $j = 3$ (super-Burnett order) (cf. [12]). (We remind the readers that all physical quantities in this paper and their mathematical definitions are given in the Nomenclature at the end of the paper.)

In practice however the Chapman-Enskog expansion as a tool for solving the Boltzmann equation has had limited practical value. Truncation at first order yields the Navier-Stokes equations which as μ ceases to be small becomes a poor approximation to solutions of the Boltzmann equation (cf. [21, 26]). Truncation at order μ^2 yields the Burnett equations which possesses the unphysical property of yielding linearly unstable rest states (cf. [1, 5, 23, 24, 25]). Simply by expanding to the higher order will not remove this instability (cf. [31]).

In addition, the Chapman-Enskog expansion destroys the material frame indifference at the Burnett order (cf. [4]).

Despite the linear instability of the Burnett equations, numerical solutions on augmented Burnett equations (cf. [1, 11, 36]) suggest that they provide more accurate solutions in the shock layer than those of the Navier-Stokes equations when compared with the direct simulation Monte-Carlo method of the Boltzmann equation. In [1, 11, 36] the augmented Burnett equations were obtained either by removing the unstable term from or by adding linearly stabilizing terms of the super Burnett order to the stress and heat flux. Unfortunately the augmented Burnett equations possess two drawbacks. First, numerically they require resolution of the super-Burnett stabilizing terms which practically means numerical resolution of derivatives up to fourth order. This is rather a cumbersome approach in several space dimensions. Secondly, the augmented Burnett equations have not been shown to have a globally defined entropy possessing the usual property of satisfying an entropy inequality.

In [16], a visco-elastic relaxation approximation was introduced as an approximation to the Boltzmann equation. This relaxation system has the following properties.

(i) It requires at most resolution of second derivatives in spatial variables;
(ii) it possesses a globally defined "entropy" like function;
(iii) when expanded via the Chapman-Enskog expansion, it matches the classical Chapman-Enskog expansion for the Boltzmann equation to the Burnett order.

Specifically the pressure deviator and heat flux were relaxed by rate equations to obtain a system of local equations that can recover the Burnett equations via the Chapman-Enskog expansion

with a correction at the super-Burnett order. By doing this, a system of thirteen local equations were obtained that is linearly stable. This system is weakly parabolic with a linearly hyperbolic convection part. Moreover, it is endowed with a generalized entropy inequality. The nonlinear entropy inequality guarantees the irreversibility of the relaxation process. The localness of this system is attractive for a robust numerical approximation to the gas dynamics valid to the Burnett order.

In recent years, relaxation approximations have been used as an effective tool to design numerical methods — known as the relaxation schemes. In [18] a generic way to relax a general system of hyperbolic conservation laws was introduced by Jin and Xin, which induced a class of relaxation schemes free of Riemann solver and local characteristic decomposition for inviscid gas dynamics. A physically natural pressure relaxation method was developed by Coquel and Perthame for an inviscid general gas[9].

In this paper, for one-dimensional problem, we propose a class of relaxation schemes for the Boltzmann equation based on the relaxed Burnett system by Jin and Slemrod. There are two main difficulties when discretizing this system. First, the equations for the stress deviator and heat flux are not in conservative form, thus canonical shock capturing methods, developed by hyperbolic systems of conservation laws, cannot be applied directly. Secondly, the stiff relaxation terms need to be discretized properly so the scheme is efficient even for small mean free paths.

Our relaxation schemes combine a conservative solver for the conserved part of the system (balance laws for density, momentum and energy), while for equations of $\boldsymbol{P}$ and $\boldsymbol{q}$ we discretize the spatial derivatives using slope limiters and central differences. These discretizations are carried out conveniently using a staggered grid, as in a staggered non-oscillatory central scheme.

We compare the numerical results obtained by this relaxation scheme with those obtained by DSMC, the Navier-Stokes equations and the extended thermodynamics (with thirteen moments) for one-dimensional stationary shocks with various Mach numbers. Our results show that the relaxed Burnett system offers more accurate shock profiles compared to the DSMC than other hydrodynamic theories.

The paper is divided into five sections after this Introduction. Section 2 reviews the relaxed Burnett system introduced by Jin and Slemrod. We also derive boundary conditions for this system using the moment definition from the probability density distribution. Section 3 reviews several main properties of the relaxed Burnett system, and computes the linear dispersion relation. In Section 4 we introduce the numerical discretization for the one-dimensional relaxed Burnett system. In section 5 we solve a one-dimensional stationary shock problem by the newly introduced relaxation scheme, and compare it with DSMC, Navier-Stokes and extended thermodynamics. We end the paper with a few concluding remarks in Section 6.

2 The Relaxed Burnett System

2.1 The Field Equations of Balance

The field equations of balance for continuum fluid dynamics in the absence of heat sources are as follows

$$\dot{\rho} + \rho \operatorname{div} \boldsymbol{u} = 0 \qquad \text{(mass conservation)}, \tag{1}$$

$$\rho \dot{\boldsymbol{u}} + \operatorname{grad} p + \operatorname{div} \boldsymbol{P} = \rho \boldsymbol{b} \qquad \text{(linear momentum conservation)}, \tag{2}$$

$$\boldsymbol{P} = \boldsymbol{P}^T \qquad \text{(rotational momentum conservation)}, \tag{3}$$

$$\rho \dot{\mathrm{e}} + p \operatorname{div} \boldsymbol{u} + \boldsymbol{P} \cdot \boldsymbol{S} + \operatorname{div} \boldsymbol{q} = 0 \qquad \text{(energy conservation)}, \tag{4}$$

where

$$\mathrm{e} = \psi - \theta\frac{\partial\psi}{\partial\theta}, \qquad \eta = -\frac{\partial\psi}{\partial\theta}, \qquad p = \rho^2\frac{\partial\psi}{\partial\rho}. \tag{5}$$

Differentiation of the expression for the Helmholtz free energy $\psi = \varepsilon - \theta\eta$ yields

$$\rho\,\theta\,\dot{\eta} = \rho\,\dot{e} - \rho\,\dot{\rho}\,\frac{\partial\psi}{\partial\rho},$$

which when combined with (1) and (4), yields the entropy production equation

$$\rho\,\theta\,\dot{\eta} = -\boldsymbol{P}\cdot\boldsymbol{S} - \operatorname{div}\boldsymbol{q}. \tag{6}$$

Division by θ yields the total entropy product rate of a fluid occupying domain $\mathcal{B} \subset \mathbb{R}^3$

$$\frac{d}{dt}\int_{\mathcal{B}}\rho\,\eta\,dV = -\int_{\mathcal{B}}\frac{\boldsymbol{P}\cdot\boldsymbol{S}}{\theta} + \frac{\boldsymbol{q}\cdot\operatorname{grad}\theta}{\theta^2}\,dV - \int_{\partial\mathcal{B}}\frac{\boldsymbol{q}\cdot\boldsymbol{n}}{\theta}\,dA. \tag{7}$$

The Clausius-Duhem inequality is a common albeit not universally accepted form of the second law of thermodynamics. It asserts

$$\frac{d}{dt}\int_{\mathcal{B}}\rho\,\eta\,dV + \int_{\partial\mathcal{B}}\frac{\boldsymbol{q}\cdot\boldsymbol{n}}{\theta}\,dA \geq 0,$$

which in turn from (7) requires $\boldsymbol{P}, \boldsymbol{q}$ to satisfy

$$\int_{\mathcal{B}}\frac{\boldsymbol{P}\cdot\boldsymbol{S}}{\theta} + \frac{\boldsymbol{q}\cdot\operatorname{grad}\theta}{\theta^2}\,dV \leq 0$$

for all fluid domains $\mathcal{B}$. However the classical Clausius-Duhem inequality is inconsistent with $\boldsymbol{P}, \boldsymbol{q}$ delivered by the Chapman-Enskog expansion beyond Navier-Stokes order.

2.2 The Chapman-Enskog Expansion

The Chapman-Enskog expansion for a monatomic gas of spherical molecules yields the constitutive relations

$$\mathrm{e} = \frac{3}{2}R\,\theta, \qquad p = R\rho\,\theta, \qquad \mu = \mu(\theta), \tag{8}$$

$$\psi = R\,\theta\,\log\,\rho - \frac{3}{2}R\,\theta\,\log\,\theta + \frac{3}{2}R\,\theta - a\,\theta + b, \tag{9}$$

$$\eta = -R\,\log\,\rho + \frac{3}{2}R\,\log\,\theta + a. \tag{10}$$

where a, b are constants of integration.

In addition the expansion provides representations for the pressure deviator tensor $\boldsymbol{P}$ and heat flux vector $\boldsymbol{q}$ in terms of a series which may be ordered via powers of the viscosity μ in terms of the total number of space plus time derivatives. Following the notation of Ferziger and Kaper[10] we record

$$\boldsymbol{P} = \mu\boldsymbol{P}^{(1)} + \mu^2\boldsymbol{P}^{(2)} + \cdots, \tag{11}$$

$$\boldsymbol{q} = \mu\boldsymbol{q}^{(1)} + \mu^2\boldsymbol{q}^{(2)} + \cdots, \tag{12}$$

where the expressions for $\boldsymbol{P}^{(1)}, \boldsymbol{P}^{(2)}, \boldsymbol{q}^{(1)}, \boldsymbol{q}^{(2)}$ are as follows

$$\boldsymbol{P}^{(1)} = -2\boldsymbol{S}, \tag{13}$$

$$\boldsymbol{q}^{(1)} = -\frac{3}{2}\mathcal{M}R\operatorname{grad}\theta, \tag{14}$$

$$\begin{aligned}\boldsymbol{P}^{(2)} =&\omega_1\frac{1}{p}(\operatorname{div}\boldsymbol{u})\boldsymbol{S}+\omega_2\frac{1}{p}\Big\{\dot{\boldsymbol{S}}-\boldsymbol{L}\boldsymbol{S}-\boldsymbol{S}L^T+\frac{2}{3}\operatorname{tr}(\boldsymbol{S}L^T)\boldsymbol{I}\Big\}+\omega_3\frac{1}{\rho\,\theta}\Big\{\operatorname{grad}^2\theta-\frac{1}{3}\Delta\theta\boldsymbol{I}\Big\}\\ &+\omega_4\frac{1}{\rho\,p\,\theta}\Big\{\frac{1}{2}\operatorname{grad}p\otimes\operatorname{grad}\theta+\frac{1}{2}\operatorname{grad}\theta\otimes\operatorname{grad}p-\frac{1}{3}\operatorname{grad}p\cdot\operatorname{grad}\theta\boldsymbol{I}\Big\}\\ &+\omega_5\frac{1}{\rho\,\theta^2}\Big\{\operatorname{grad}\theta\otimes\operatorname{grad}\theta-\frac{1}{3}|\operatorname{grad}\theta|^2\boldsymbol{I}\Big\}+\omega_6\frac{1}{p}\Big\{\boldsymbol{S}^2-\frac{1}{3}\operatorname{tr}(\boldsymbol{S}^2)\boldsymbol{I}\Big\},\end{aligned} \tag{15}$$

$$\begin{aligned}\boldsymbol{q}^{(2)} =&\theta_1\frac{1}{\rho\,\theta}(\operatorname{div}\boldsymbol{u})\operatorname{grad}\theta+\theta_2\frac{1}{\rho\,\theta}\big((\operatorname{grad}\theta)^{\bullet}-\boldsymbol{L}^T\operatorname{grad}\theta\big)\\ &+\theta_3\frac{1}{p\,\rho}(\boldsymbol{S}\operatorname{grad}p)+\theta_4\frac{1}{\rho}\operatorname{div}\boldsymbol{S}+\theta_5\frac{1}{\rho\,\theta}\boldsymbol{S}\operatorname{grad}\theta.\end{aligned} \tag{16}$$

One drawback of the Chapman-Enskog expansion is that, if truncated at the Burnett or higher order, it destroys the property of material frame indifference. In particular, in (15) and (16), the ω_2 term in $\boldsymbol{P}^{(2)}$ and the θ_2 term in $\boldsymbol{q}^{(2)}$ are both material frame dependent. It cannot be recovered by replacing the material derivative with the space derivative using the Euler or Navier-Stokes equations[4].

The coefficients $\omega_1,\cdots,\omega_6,\theta_1,\cdots,\theta_5$ are functions of θ and are not independent. For a gas of spherical molecules the following universal relations have been derived by Truesdell and Muncaster[36] generalizing more specialized relations:

$$\begin{aligned}&\omega_3=\theta_4,\\ &\theta_1=\frac{2}{3}\Big(\frac{7}{2}-\frac{\mu'(\theta)}{\mu(\theta)}\theta\Big)\theta_2-\frac{1}{3}\theta\frac{\partial\theta_2}{\partial\theta},\\ &\omega_1=\frac{2}{3}\Big(\frac{7}{2}-\frac{\mu'(\theta)}{\mu(\theta)}\theta\Big)\omega_2-\frac{1}{3}\theta\frac{\partial\omega_2}{\partial\theta}.\end{aligned} \tag{17}$$

Furthermore for gases of ideal spheres in which the collisions are purely elastic or satisfy an inverse k^{th}-power attraction between molecules, the coefficients $\omega_1,\omega_2,\cdots,\theta_5$ are independent of θ. In addition the relations

$$\frac{\theta_1}{\theta_2}=\frac{\omega_1}{\omega_2}=\begin{cases}\dfrac{2}{3}\Big(\dfrac{3k-5}{k-1}\Big) & \text{for inverse } k^{\text{th}} \text{ power molecules,}\\ 2 & \text{for ideal spheres}\end{cases}$$

hold.

Exact determination of $\omega_1,\omega_2,\cdots,\theta_5$ has only been accomplished for a gas of Maxwellian ($k=5$) molecules. For the more general case only approximations to $\omega_1,\omega_2,\cdots,\theta_5$ have been obtained. The classical approximation result (say as found in [10, p.149]) is

$$\begin{aligned}&\omega_2\simeq 2,\quad \omega_3\simeq 3,\quad \omega_4\simeq 0,\quad \omega_5\simeq\frac{\mu'(\theta)\,\theta\,\omega_3}{\mu(\theta)},\quad \omega_6\simeq 8,\\ &\theta_2\simeq\frac{45}{8},\quad \theta_3\simeq -3,\quad \theta_4\simeq 3,\quad \theta_5\simeq 3\Big(\frac{35}{4}+\frac{\theta}{\mu}\mu'(\theta)\Big),\quad \mathcal{M}\simeq\frac{5}{2}.\end{aligned} \tag{18}$$

For Maxwell molecules the relations (18) are exact

$$\frac{\theta_1}{\theta_2}=\frac{\omega_1}{\omega_2}=\frac{5}{3},\qquad \frac{\theta\mu'(\theta)}{\mu(\theta)}=1,$$

and μ is linear in θ.

In this paper we shall assume that in addition to (17) the following relations hold

$$\begin{aligned} &\theta_3+\omega_3+\omega_4=0, \qquad \omega_5=\frac{\mu'(\theta)\,\theta}{\mu(\theta)}\omega_3, \qquad \theta_5=\overline{\theta}_5+\frac{\mu'(\theta)\,\theta}{\mu(\theta)}\omega_3,\\ &\omega_3>0, \qquad \theta_2>0, \qquad \overline{\theta}_5>0, \qquad \overline{\theta}_5 \text{ a constant.} \end{aligned} \tag{19}$$

Notice the assumption (19) holds for the approximation (18) but does not assume the molecules are ideal spheres or satisfy an inverse k^{th} power attraction law. Of course (17), (19) are satisfied by Maxwell molecules. However we reiterate the fact that relation (17) and the first equation in (19) are universal for all spherical molecules (cf. [34]).

2.3 The Relaxation Approximation

Since it is the material derivative terms on the right hand side of (15) and (16) that introduce the linear instability[33], a relaxation approximation that regularizes $\bar{\boldsymbol{P}}$ and $\boldsymbol{q}$ was introduced by Jin and Slemrod in [16]. There rate type relaxation equations for $\bar{\boldsymbol{P}}$ and $\boldsymbol{q}$, in the spirit of viscoelastic fluids, were introduced. The resulting relaxed Burnett system for $\rho, \boldsymbol{u}, e, \boldsymbol{P}$ and $\boldsymbol{q}$ take the following form:

$$\dot{\rho}+\rho\,\mathrm{div}\,\boldsymbol{u}=0, \tag{20}$$

$$\rho\dot{\boldsymbol{u}}+\mathrm{grad}\,p+\mathrm{div}\,\boldsymbol{P}=\rho\boldsymbol{b}, \tag{21}$$

$$\boldsymbol{P}=\boldsymbol{P}^T, \tag{22}$$

$$\dot{\boldsymbol{P}}-\boldsymbol{L}\boldsymbol{P}-\boldsymbol{P}\boldsymbol{L}^T+\frac{2}{3}\,\mathrm{tr}\,(\boldsymbol{P}\boldsymbol{L}^T)\,\boldsymbol{I}=-\frac{2p}{\omega_2\mu}(\boldsymbol{P}-\boldsymbol{P}^{eq}), \tag{23}$$

$$\rho\,\dot{\mathrm{e}}+p\,\mathrm{div}\,\boldsymbol{u}+\boldsymbol{P}\cdot\boldsymbol{S}+\mathrm{div}\,\boldsymbol{q}=0, \tag{24}$$

$$\dot{\boldsymbol{q}}-\boldsymbol{L}^T\boldsymbol{q}=-\frac{3\mathcal{M}p}{2\,\theta_2\,\mu}(\boldsymbol{q}-\boldsymbol{q}^{eq}), \tag{25}$$

where

$$\boldsymbol{P}^{eq}=-2\mu\boldsymbol{S}+\boldsymbol{P}_2+\boldsymbol{P}_3, \tag{26}$$

with

$$\begin{aligned} \boldsymbol{P}_2=&-\mu\frac{\omega_1}{2p}(\mathrm{div}\,\boldsymbol{u})\bar{\boldsymbol{P}}+\frac{\omega_2\,\mu'(\theta)\,\dot{\theta}}{2p}\bar{\boldsymbol{P}}+\mu^2\frac{\omega_3}{\rho\,\theta}\Big\{-\mathrm{grad}\,\Big(\frac{\boldsymbol{q}}{\frac{3}{2}\mu\mathcal{M}R}\Big)+\frac{1}{3}\,\mathrm{div}\Big(\frac{\boldsymbol{q}}{\frac{3}{2}\mu\mathcal{M}R}\Big)\boldsymbol{I}\Big\}\\ &+\mu\frac{\omega_4}{\rho\,p\,\theta}\Big\{-\frac{1}{2}\,\mathrm{grad}\,p\otimes\Big(\frac{\boldsymbol{q}}{\frac{3}{2}\mathcal{M}R}\Big)-\frac{1}{2}\Big(\frac{\boldsymbol{q}}{\frac{3}{2}\mathcal{M}R}\Big)\otimes\mathrm{grad}\,p+\frac{1}{3}\mathrm{grad}\,p\cdot\Big(\frac{\boldsymbol{q}}{\frac{3}{2}\mathcal{M}R}\Big)\boldsymbol{I}\Big\}\\ &-\mu\frac{\omega_5}{\rho\,\theta^2}\Big\{\frac{1}{2}\,\mathrm{grad}\,\theta\otimes\Big(\frac{\boldsymbol{q}}{\frac{3}{2}\mathcal{M}R}\Big)+\frac{1}{2}\Big(\frac{\boldsymbol{q}}{\frac{3}{2}\mathcal{M}R}\Big)\otimes\mathrm{grad}\,\theta+\frac{1}{3}\,\mathrm{grad}\,\theta\cdot\Big(\frac{\boldsymbol{q}}{\frac{3}{2}\mathcal{M}R}\Big)\boldsymbol{I}\Big\}\\ &-\mu\frac{\omega_6}{2p}\Big\{\frac{1}{2}(\boldsymbol{S}\boldsymbol{P}+\boldsymbol{P}\boldsymbol{S})-\frac{1}{3}\,\mathrm{tr}\,(\boldsymbol{P}\boldsymbol{S})\,\boldsymbol{I}\Big\}, \end{aligned} \tag{27}$$

$$\boldsymbol{P}_3=\mu^2\Big[\frac{\widehat{\omega}_2}{p^2}\,\mathrm{tr}\,\boldsymbol{S}^2+\widehat{\omega}_3\frac{|\mathrm{grad}\,\theta|^2}{R\,\rho^2\theta^3}\Big]\boldsymbol{P}+\mu\frac{\widehat{\gamma}_1}{p\,\theta}\Big(\dot{\theta}+\frac{2}{3}\theta\,\mathrm{div}\,\boldsymbol{u}\Big)\boldsymbol{P}+\widehat{\omega}_4\Big[\frac{\mu^3}{\mathcal{M}R\,\rho^2}\Big(\frac{1}{2\mu\,\theta}P^{ij}\Big)_{,k}\Big]_{,k}, \tag{28}$$

and

$$\boldsymbol{q}^{eq}=-\frac{3}{2}\mu\mathcal{M}R\,\mathrm{grad}\,\theta+\boldsymbol{q}_2+\boldsymbol{q}_3, \tag{29}$$

with

$$\begin{aligned}\boldsymbol{q}_2 =& -2\mu\frac{\theta_1}{3\mathcal{M}R\,\rho\,\theta}(\operatorname{div}\boldsymbol{u})\boldsymbol{q}+\frac{2\theta_2\dot\theta\mu'(\theta)}{3\mathcal{M}R\,\rho\,\theta}\boldsymbol{q}-\mu\frac{\theta_3}{2p\,\rho}\boldsymbol{P}\operatorname{grad}p\\ &-\mu^2\frac{\theta_4}{2\rho}\operatorname{div}\Big(\frac{\boldsymbol{P}}{\mu}\Big)-\mu\frac{\theta_5}{2\rho\,\theta}\boldsymbol{P}\operatorname{grad}\theta, \qquad (30)\\ \boldsymbol{q}_3 =&\mu^2\Big[\frac{\widehat\theta_2}{p^2}\operatorname{tr}\boldsymbol{S}^2+\widehat\theta_3\frac{|\operatorname{grad}\theta|^2}{R\rho^2\theta^3}\Big]\boldsymbol{q}+\mu\frac{\widehat\lambda_1}{\rho\,\theta^2}\Big(\dot\theta+\frac{2}{3}\,\theta\operatorname{div}\boldsymbol{u}\Big)\Big(\frac{\boldsymbol{q}}{\frac{3}{2}\mathcal{M}R}\Big)\\ &+\widehat\theta_4\Big[\frac{\mu^3\theta}{\rho^2}\Big(\frac{2}{3\mathcal{M}R\,\mu\,\theta^2}\,q_i\Big)_{,k}\Big]_{,k}. \qquad (31)\end{aligned}$$

In (28) and (31) conventional summation notation is used. Since the energy equation (24) implies that

$$\dot\theta+\frac{2}{3}\,\theta\operatorname{div}\boldsymbol{u}=\frac{2}{3\rho\,R}(-\boldsymbol{P}\cdot\boldsymbol{S}-\operatorname{div}\boldsymbol{q}), \qquad (32)$$

system (20)–(25) is weakly parabolic and local (does not contain $\dot\theta$ on the right hand side) after using (31). Moreover, (31) suggests that $\dot\theta+\frac{2}{3}\theta\operatorname{div}\boldsymbol{u}=O(\mu)$, and $\boldsymbol{P}_3$ and $\boldsymbol{q}_3$ are $O(\mu^3)$, thus belong to the super Burnett order. It is a trivial observation that (20)–(25) yield a representation of $\boldsymbol{P}$, $\boldsymbol{q}$ in powers of μ, which agrees with the classical Burnett equations, i.e., terms of order μ^2 from the Chapman-Enskog expansion of the Boltzmann equation, with corrections at $O(\mu^3)$. Yet unlike the augmented Burnett systems of [1, 11, 36] the system possesses spatial derivatives only up to the second order.

2.4 Boundary Conditions

The Chapman-Enskog expansion in itself prescribes no boundary conditions. We can derive the boundary conditions if we associate density ρ, velocity $\boldsymbol{u}$, stress deviator $\boldsymbol{P}$ and heat flux $\boldsymbol{q}$ with their relations defined by the moment of probability density distribution.

Consider the probability density distribution $f(\boldsymbol{x},,\boldsymbol{\xi})$, solution of the Boltzmann equation. Let $\boldsymbol{c}=\boldsymbol{\xi}-\boldsymbol{u}$ be the peculiar velocity. Then the connection between f and the macroscopic quantities are established by the moments:

$$\begin{aligned}&\rho=\int_{\mathbb{R}^3}f\,d\boldsymbol{\xi}, \qquad \rho\boldsymbol{u}=\int_{\mathbb{R}^3}f\boldsymbol{\xi}\,d\boldsymbol{\xi},\\ &P_{ij}=\int_{\mathbb{R}^3}c_ic_jf\,d\boldsymbol{\xi}, \quad i\neq j, \qquad q_i=\frac{1}{2}\int_{\mathbb{R}^3}c_i|\boldsymbol{c}|^2f\,d\boldsymbol{\xi},\end{aligned} \qquad (33)$$

Now following [13], we consider for simplicity the boundary perpendicular to the x_1-axis with specular reflective boundary conditions:

$$f(\boldsymbol{\xi})=f^+(\boldsymbol{\xi})+f^-(\boldsymbol{\xi}), \qquad (34)$$

$$f^+(\boldsymbol{\xi})=0 \quad \text{for } \xi_1<0, \qquad f^-(\boldsymbol{\xi})=0 \quad \text{for } \xi_1>0, \qquad (35)$$

$$f^+(\xi_1,\xi_2,\xi_3)=f^-(-\xi_1,\xi_2,\xi_3). \qquad (36)$$

This is of course equivalent to the statement that f is even in ξ_1. Hence

$$\rho u_1=\int_{\mathbb{R}^3}\xi_1f\,d\,\xi_1\xi_2\xi_3,$$

being the integral of an odd function on $-\infty<\xi_1<\infty$ must vanish and hence $u_1=0$ on the boundary, i.e., $\boldsymbol{u}\cdot\boldsymbol{n}=0$, where $\boldsymbol{n}$ is the unit normal to the boundary. Since $u_1=0$ on the boundary, $c_1=\xi_1$, thus $q_1=0$, $P_{12}=P_{13}=0$ as well. Hence we have $\boldsymbol{q}\cdot\boldsymbol{n}=0$.

$\boldsymbol{Pn}$ delivers the tractions on the surface which in our case is $\boldsymbol{Pn} = (P_{11}, P_{12}, P_{13})$ and hence the surface traction is parallel to the surface normal $\boldsymbol{n}$, i.e., $\boldsymbol{Pn} \times \boldsymbol{n} = \boldsymbol{0}$.

Since for a smooth surface we may locally arrange the coordinates so that the surface is locally perpendicular to the x_1 axis, Grad's conditions for specularly reflective boundary condition for an arbitrary smooth surface are simply $\boldsymbol{u} \cdot \boldsymbol{n} = 0,\ \boldsymbol{q} \cdot \boldsymbol{n} = 0,\ \boldsymbol{Pn} \times \boldsymbol{n} = \boldsymbol{0}$, where $\boldsymbol{n}$ is a normal to the surface.

3 Properties of the Relaxed Burnett System

To make the paper more complete we review in this section two main properties of the relaxed Burnett equations, namely, the global generalized entropy inequality and the (local) hyperbolicity of the linearized system. Both were proved in [16]. We also give the linear dispersion relation.

3.1 Generalized Entropy Inequality

Under certain assumptions the following generalized entropy inequality for the relaxation systems (20)–(26)can be established. This inequality guarantees the irreversibility of the relaxation process. In addition to the classical entropy for the Navier-Stokes equations, the generalized entropy also depends on the nonequilibrium variables $\boldsymbol{P}$ and $\boldsymbol{q}$.

Theorem 3.1. *Let $\boldsymbol{P}$,$\boldsymbol{q}$ be given by (20)–(31) with*

$$\widehat{\lambda}_1 = -\frac{1}{2}\,\theta\,\frac{\partial \theta_2}{\partial \theta} - \theta_2 \theta\,\frac{\mu'(\theta)}{\mu(\theta)} + \frac{3}{2}\,\theta_2, \tag{37}$$

$$\widehat{\gamma}_1 = -\frac{1}{2}\,\theta\,\frac{\partial \omega_2}{\partial \theta} - \omega_2\,\theta\,\frac{\mu'(\theta)}{\mu(\theta)} + \omega_2, \tag{38}$$

in (28), (31) respectively.

Assume that $\widehat{\omega}_4 \geq 0,\ \widehat{\theta}_4 \geq 0$. Furthermore, define $\boldsymbol{z} \in \mathbb{R}^5$ by

$$\boldsymbol{z} = \left[\Big(\frac{\operatorname{tr}\boldsymbol{P}^2}{\theta}\Big)^{1/2},\ \sqrt{\frac{2}{3}}\,\frac{|\boldsymbol{q}|}{\sqrt{\mathcal{M}R}\,\theta},\ \mu\frac{(\operatorname{tr}\boldsymbol{S}^2\operatorname{tr}\boldsymbol{P}^2)^{1/2}}{p(R\theta)^{1/2}},\ \mu\sqrt{\frac{2}{3}}\,\frac{(\operatorname{tr}\boldsymbol{S}^2)^{1/2}|\boldsymbol{q}|}{p\,\theta(\mathcal{M}R)^{1/2}},\ \sqrt{\frac{2}{3}}\,\frac{|\operatorname{grad}\theta|\,|\boldsymbol{q}|}{p\,\theta^{3/2}}\right],$$

then the following entropy inequality holds:

$$\begin{aligned}
&\rho\Big\{-\eta + \frac{1}{2}\operatorname{tr}\Big(\frac{\omega_2\boldsymbol{P}^2}{4\rho\,p\,\theta}\Big) + \frac{1}{3\mathcal{M}R}\Big(\frac{2\,\theta_2|\boldsymbol{q}|^2}{3\mathcal{M}R\rho^2\theta^3}\Big)\Big\}^{\bullet} + \operatorname{div}\Big\{\frac{\boldsymbol{q}}{\theta} + \frac{\omega_3\boldsymbol{P}\boldsymbol{q}}{3\mathcal{M}R\rho\,\theta^2}\Big\}\\
&-\widehat{\omega}_4\frac{\partial}{\partial x_k}\Big[\frac{\mu^3}{\mathcal{M}R\rho^2}\,\frac{1}{2\mu\,\theta}P^{ij}\Big(\frac{1}{2\mu\,\theta}P^{ij}\Big)_{,k}\Big] - \widehat{\theta}_4\frac{\partial}{\partial x_k}\Big[\frac{\mu^3}{\rho^2}\Big(\frac{2}{3\mathcal{M}R\mu\,\theta}\Big)q_i\Big(\frac{2}{3\mathcal{M}R\mu\,\theta}q_i\Big)_{,k}\Big]\\
&\leq -\frac{1}{\mu}\,\boldsymbol{z}\cdot\boldsymbol{D}\boldsymbol{z},
\end{aligned} \tag{39}$$

where

$$\boldsymbol{D} = \begin{bmatrix}
\frac{1}{2} & 0 & \frac{-|\omega_6 - 2\omega_2|}{8\sqrt{2}} & 0 & -\frac{|-\overline{\theta}_5 - \omega_3 + \theta\,\omega_3'(\theta)|}{\sqrt{6}\,\mathcal{M}}\\
0 & 1 & 0 & -\frac{1}{3\mathcal{M}} & 0\\
-\frac{|\omega_6 - 2\omega_2|}{8\sqrt{2}} & 0 & -\widehat{\omega}_2 & 0 & 0\\
0 & -\frac{1}{3\mathcal{M}} & 0 & -\widehat{\theta}_2 & 0\\
-\frac{|-\overline{\theta}_5 - \omega_3 + \theta\,\omega_3'(\theta)|}{\sqrt{6}\,\mathcal{M}} & 0 & 0 & 0 & -\frac{\widehat{\theta}_3}{\mathcal{M}}
\end{bmatrix}.$$

D *is positive definite if* $\widehat{\omega}_2 < 0$, $\widehat{\theta}_2 < 0$, $\widehat{\theta}_3 < 0$ *are sufficiently large in absolute value,* $\widehat{\omega}_3 \le 0$, *and* $\big| -\overline{\theta}_5 - \omega_3 + \theta\omega_3'(\theta)\big|$, $|\omega_6 - 2\omega_3|$ *are bounded.*

Remark 3.1. *In the above Theorem the positive definiteness of D is a sufficient condition but may not be necessary. The necessary condition to obtain the entropy inequality remains an open problem.*

Remark 3.2. *If* $\widehat{\omega}_4 = \widehat{\theta}_4 = 0$, *namely, the dissipative terms in* $\boldsymbol{P}_3$ *and* $\boldsymbol{q}_3$ *are not present, the entropy condition still holds and the entropy and the entropy flux in (39) agree with those of Grad's thirteen moment theory*[26]. *The generalized entropy, as in Grad's theory, is not globally convex. However, it is locally convex around the equilibrium solution (*ρ *and* θ *are constants), thus the rest state (*$u = 0$*) is stable, in contrast to the Burnett equations where the rest state is unstable.*

3.2 Hyperbolicity

The hyperbolicity of the relaxation approximation (20)–(25), when the parabolic terms are omitted, was proved in [16] in one-dimension for rest state. To reduce the system to the one dimensional case, which will be used in our numerical experiments, we assume that all quantities depend on x only, $\boldsymbol{u} = \big(u(x,), 0, 0\big)$ and look for special solution $P^{23} = P^{13} = P^{12} = q_2 = q_3 = 0$. It is easy to show that these are exact solutions to (23) and (25). Furthermore, one can show that $P^{22} = P^{33}$ is also consistent with (23) and (25). Since $\boldsymbol{P}$ has zero trace, this implies that

$$P^{22} = -\frac{1}{2}P^{11}.$$

Thus we are left with five independent variables $\rho, u, \theta, P^{11} = \sigma$ and $q_1 = q$, satisfying the system

$$\rho_+ u\rho_x + \rho u_x = 0, \tag{40}$$

$$u_+ uu_x + \frac{1}{\rho}p_x + \frac{1}{\rho}\sigma_x = 0, \tag{41}$$

$$\theta_+ u\,\theta_x + \frac{2p}{3\rho R}u_x + \frac{2}{3\rho R}\sigma u_x + \frac{2}{3\rho R}q_x = 0, \tag{42}$$

$$\sigma_+ u\sigma_x - \frac{4}{3}\sigma u_x = -\frac{2p}{\omega_2\mu}(\sigma - \sigma_{eq}), \tag{43}$$

$$q_+ uq_x - qu_x = -\frac{3\mathcal{M}p}{2\,\theta_2\mu}(q - q_{eq}), \tag{44}$$

where

$$\sigma_{eq} = -\frac{4}{3}\mu\, u_x + \sigma_2 + \sigma_3, \tag{45}$$

with

$$\begin{aligned}\sigma_2 =& -\mu\frac{\omega_1}{2p}\sigma u_x + \frac{\omega_2\mu'(\theta)\,\dot{\theta}}{2p}\sigma - \mu^2\frac{4\omega_3}{9\rho\,\theta}\Big(\frac{q}{\mu\mathcal{M}R}\Big)_x - \mu\frac{4\omega_4}{9\rho\,p\,\theta}\,\frac{q}{\mathcal{M}R}\,p_x \\ & - \mu\frac{4\omega_5}{9\rho\,\theta^2}\,\frac{q}{\mathcal{M}R}\theta_x - \mu\frac{\omega_6}{6p}\sigma u_x,\end{aligned} \tag{46}$$

$$\sigma_3 = \mu^2\Big[\frac{2\widehat{\omega}_2}{3p^2}\,{u_x}^2 + \widehat{\omega}_3\frac{{\theta_x}^2}{R\rho^2\theta^3}\Big]\sigma - \mu\frac{\widehat{\gamma}_1}{p\,\theta}\,\frac{2}{3\rho R}(\sigma^2 u_x + \sigma q_x) + \widehat{\omega}_4\Big[\frac{\mu^3}{\mathcal{M}R\rho^2}\Big(\frac{\sigma}{2\mu\,\theta}\Big)_x\Big]_x, \tag{47}$$

and

$$q_{eq} = -\frac{3}{2}\,\mu\mathcal{M}R\,\theta_x + q_2 + q_3 \tag{48}$$

with

$$q_2 = -2\mu\frac{\theta_1}{3\mathcal{M}R\,\rho\,\theta}qu_x + \frac{2\theta_2\dot{\theta}\mu'(\theta)}{3\mathcal{M}R\rho\,\theta}q - \mu\frac{\theta_3}{2p\,\rho}\sigma p_x - \mu^2\frac{\theta_4}{2\rho}\Big(\frac{\sigma}{\mu}\Big)_x - \mu\frac{\theta_5}{2\rho\,\theta}\sigma\theta_x, \tag{49}$$

$$\begin{aligned} q_3 =& \mu^2\Big[\frac{2\widehat{\theta}_2}{3p^2}{u_x}^2 + \widehat{\theta}_3\frac{{\theta_x}^2}{R\rho^2\theta^3}\Big]q - \mu\frac{\widehat{\lambda}_1}{\rho\,\theta^2}\,\frac{2}{3\rho R}(\sigma u_x + q_x)\Big(\frac{q}{\frac{3}{2}\mathcal{M}R}\Big) \\ &+ \widehat{\theta}_4\Big[\frac{\mu^3\theta}{\rho^2}\Big(\frac{2}{3\mathcal{M}R\,\mu\,\theta^2}q\Big)_x\Big]_x. \end{aligned} \tag{50}$$

Set $\widehat{\omega}_4 = \widehat{\theta}_4 = 0$. Upon using $p = R\rho\theta$, and (42) to replace $\dot{\theta}$, one obtains the Jacobi matrix for the relaxation system (40)–(44)

$$\boldsymbol{J} = \begin{bmatrix} u & \rho & 0 & 0 & 0 \\ \dfrac{R\,\theta}{\rho} & u & R & \dfrac{1}{\rho} & 0 \\ 0 & J_{32} & u & 0 & \dfrac{2}{3R\rho} \\ J_{41} & J_{42} & J_{43} & u & J_{46} \\ J_{51} & J_{52} & J_{53} & J_{54} & J_{56} \end{bmatrix}, \tag{51}$$

where for Maxwellian molecules

$$J_{32} = \frac{2}{3}\,\theta + \frac{2}{3R\rho}\sigma, \tag{52}$$

$$J_{41} = 0, \quad J_{42} = \frac{7}{3}\sigma + \frac{4}{3}p + \frac{2}{3}\,\frac{\sigma^2}{p}, \quad J_{43} = 0, \quad J_{46} = \frac{2}{3}\,\frac{\sigma}{p} + \frac{8}{15}, \tag{53}$$

$$J_{51} = -\frac{p}{\rho^2}\sigma, \quad J_{52} = \frac{q}{p}\sigma + \frac{4}{3}q, \quad J_{53} = \frac{5}{2}\,pR + \frac{31}{4}R\sigma, \quad J_{54} = \frac{p}{\rho}, \quad J_{56} = u + \frac{q}{p}, \tag{54}$$

while the characteristic polynomial becomes (upon changing $u - \lambda \to -\lambda$)

$$\lambda[\lambda^4 + a_3\lambda^3 + a_2\lambda^2 + a_1\lambda + a_0], \tag{55}$$

with the coefficients

$$\begin{aligned} a_0 =& \frac{123}{10}\,\frac{P\sigma}{\rho^2} + 3\,\frac{p^2}{\rho^2} + \frac{587}{90}\,\frac{\sigma^2}{\rho^2}, \qquad a_1 = \frac{7}{5}\,\frac{q}{\rho} + \frac{41}{45}\,\frac{q\sigma}{p\rho}, \\ a_2 =& -\frac{26}{5}\,\frac{p}{\rho} - \frac{53}{6}\,\frac{\sigma}{\rho} - \frac{2}{3}\,\frac{\sigma^2}{p\rho}, \qquad a_3 = -\frac{q}{p}. \end{aligned}$$

Linearizing system (40)–(44) around the rest state ($\overline{\rho}$, 0, $\overline{\theta}$, 0, 0), where $\overline{\rho}$, $\overline{\theta}$ are constants. In this case, the characteristic polynomial (55) reduces to

$$\lambda\Big[\lambda^4 - \frac{26}{5}\,\frac{\overline{p}}{\overline{\rho}}\,\lambda^2 + 3\Big(\frac{\overline{p}}{\overline{\rho}}\Big)^2\Big],$$

where $\overline{p} = R\overline{\theta}\overline{\rho}$. This polynomial has been shown in [16] to have five distinct roots

$$0, \quad \pm\sqrt{\frac{13}{5} \pm \sqrt{\frac{94}{25}}}\,\sqrt{\frac{\overline{p}}{\overline{\rho}}}.$$

Thus the linearized relaxation system, when the parabolic terms are omitted, is hyperbolic. This shows that the relaxation system is at least locally well-posed for initial value problems.

By incorporating the weakly parabolic terms this well-posedness is conjectured but remains an open problem.

3.3 Dispersion Relation

If we set $z = \frac{\overline{\rho}\, c_0^2}{\omega\, \mu},\ c_0^2 = \frac{5}{3}\, R\, \overline{\theta}$, the dispersion relation is obtained by setting $\boldsymbol{v} = (\rho, u, \theta, \sigma, q)^T$ equal to $e^{i(\omega - kx)}\boldsymbol{v}_0$ and looking for the non-trivial solution of

$$\det\Big[\frac{\omega}{k}\boldsymbol{I} - \boldsymbol{J} + \frac{i}{k}\boldsymbol{A} - i\,k\boldsymbol{B}\Big] = 0.$$

Here

$$A_{44} = -\frac{6\,\omega\, z}{5\,\omega_2}, \qquad A_{55} = -\frac{9M\omega z}{10\,\theta_2}, \qquad B_{44} = \frac{\widehat{\omega}_4\, c_0^2}{\omega_2 M\omega z}, \qquad B_{55} = \frac{\widehat{\theta}_4\, c_0^2}{\theta_2\, \omega z}.$$

Hence in the limit as $\omega \to \infty$, i.e., $z \to 0$, $A_{44} = A_{55} = 0$. If furthermore we restrict ourselves to the case with no diffusion: $\widehat{\omega}_4 = \widehat{\theta}_4 = 0$, then $\boldsymbol{B} = 0$ and we see that $\frac{\omega}{k}$ will be precisely equal to the eigenvalue of $\boldsymbol{J}$:

$$0, \quad \pm\sqrt{\frac{13}{5} \pm \sqrt{\frac{94}{25}}}\ \sqrt{\frac{\overline{p}}{\overline{\rho}}}.$$

Since $\frac{\overline{p}}{\overline{\rho}} = \frac{3}{5}c_0^2$, we have

$$\frac{\omega}{k\, c_0} = 0, \qquad \frac{\omega}{k\, c_0} = \pm\frac{\sqrt{3}}{5}\sqrt{13 \pm \sqrt{94}} = \pm 1.649\cdots, \pm 0.6294\cdots.$$

The nonzero values are identical to those obtained by Grad[13] and extended thermodynamics of 13 variables (cf. [26]).

In the case $\widehat{\theta}_4 > 0,\ \widehat{\omega}_4 > 0$, we obtain $\frac{\omega}{k\, c_0} \to \infty$ as $z \to 0$ as in the Navier-Stokes theory.

4 Numerical Schemes

4.1 Formulation and Time Splitting

We will devise a numerical scheme for one dimensional system (40)–(44). Since the system cannot be written in conservative form we use the following form to devise our numerical approximations:

$$U_+ F(U,V)_x = 0, \qquad V_+ G(U,V,U_x,V_x) = D(U,V,U_x,V_x)_x, \tag{56}$$

where

$$U = \begin{pmatrix} \rho \\ \rho\, u \\ \frac{1}{2}\rho\, u^2 + \frac{3}{2}p \end{pmatrix}, \quad V = \begin{pmatrix} \sigma \\ q \end{pmatrix}, \quad F(U,V) = \begin{pmatrix} \rho\, u \\ \rho\, u^2 + p + \sigma \\ \frac{1}{2}\rho\, u^3 + \frac{5}{2}up + \sigma u + q \end{pmatrix}, \tag{57}$$

$$G(U,V,U_x,V_x) = \begin{pmatrix} u\sigma_x - \frac{4}{3}\sigma u_x + \frac{2p}{\omega_2\mu}(\sigma - \widetilde{\sigma}_{eq}) \\ uq_x - qu_x + \frac{3\mathcal{M}p}{2\theta_2\mu}(q - \widetilde{q}_{eq}) \end{pmatrix}, \tag{58}$$

$$D(U,V,U_x,V_x)_x = \begin{pmatrix} \frac{2p}{\omega_2\mu}\widehat{\omega}_4\Big[\frac{\mu^3}{\mathcal{M}R\rho^2}\Big(\frac{\sigma}{2\mu\theta}\Big)_x\Big]_x \\ \frac{3\mathcal{M}p}{2\theta_2\mu}\widehat{\theta}_4\Big[\frac{\mu^3\theta}{\rho^2}\Big(\frac{2}{3\mathcal{M}R\mu\theta^2}q\Big)_x\Big]_x \end{pmatrix} = \begin{pmatrix} \frac{2p}{\omega_2\mu}d_1 \\ \frac{3\mathcal{M}p}{2\theta_2\mu}d_2 \end{pmatrix}, \tag{59}$$

and now

$$\widetilde{\sigma}_{eq} = -\frac{4}{3}\,\mu\, u_x + \sigma_2 + \widetilde{\sigma}_3, \qquad \widetilde{\sigma}_3 = \sigma_3 - d_1, \tag{60}$$

$$\widetilde{q}_{eq} = -\frac{3}{2}\mu\,\mathcal{M}R\,\theta_x + q_2 + \widetilde{q}_3, \qquad \widetilde{q}_3 = q_3 - d_2. \tag{61}$$

As in standard numerical methods for hyperbolic systems with relaxations, we use operator splitting by splitting the convective operators

$$U_+F(U,V)_x = 0, \qquad V_+G(U,V,U_x,V_x) = 0, \tag{62}$$

from the rest (diffusive operators and source terms)

$$U_=0, \qquad V_=D(U,V,U_x,V_x)_x. \tag{63}$$

The main advantage of this splitting is that, in the diffusion step, $U_=0$, thus the V equations can be solved with a fully implicit method — which has a good stability property — without solving nonlinear systems of algebraic equations.

4.2 Discretizations

Let us consider the convective step

$$U_+F(U,V)_x = 0, \tag{64}$$

$$V_+G(U,V,U_x,V_x) = 0. \tag{65}$$

For spatial discretizations we use a staggered grid as in [22, 28]. Define the grid points as

$$x_j = j\Delta x, \qquad x_{j+1/2} = x_j + \frac{1}{2}\Delta x, \qquad j = \cdots, -2, -1, 0, 1, 2, \cdots, \tag{66}$$

and use the standard notation for cell-averages:

$$U^{n+1}_{j+1/2} = \frac{1}{\Delta x}\int_{x_j}^{x_{j+1}} U(x,^{n+1})\,dx, \qquad V^{n+1}_{j+1/2} = \frac{1}{\Delta x}\int_{x_j}^{x_{j+1}} V(x,^{n+1})\,dx. \tag{67}$$

By integrating system (64), (65) over the cell $[x_j, x_{j+1}] \times [^n, ^{n+1}]$ one obtains

$$U^{n+1}_{j+1/2} = \frac{1}{\Delta x}\int_{x_j}^{x_{j+1}} U(x,^n)\,dx + \frac{1}{\Delta x}\int_n^{n+1} F\big(U(x_j,), V(x_j,)\big) - F\big(U(x_{j+1},), V(x_j,)\big)\,dt,$$

$$V^{n+1}_{j+1/2} = \frac{1}{\Delta x}\int_{x_j}^{x_{j+1}} V(x,^n)\,dx + \frac{1}{\Delta x}\int_n^{n+1}\int_{x_j}^{x_{j+1}} G\big(U(x,),V(x,),U_x(x,),V_x(x,)\big)\,dx\,dt.$$

At each time level $^n = n\Delta$ we approximate $U(x,^n)$ and $V(x,^n)$ by their piecewise linear approximations

$$LU_j(x,) = U_j() + (x - x_j)\frac{U'_j}{\Delta x}, \qquad x_{j-1/2} < x < x_{j+1/2}, \tag{68}$$

$$LV_j(x,) = V_j() + (x - x_j)\frac{V'_j}{\Delta x}, \qquad x_{j-1/2} < x < x_{j+1/2}, \tag{69}$$

where U'_j and V'_j are numerical derivatives such that

$$\frac{U'_j}{\Delta x} = U_x(x_j,) + O(\Delta x), \qquad \frac{V'_j}{\Delta x} = V_x(x_j,) + O(\Delta x). \tag{70}$$

Then (68) becomes

$$\begin{aligned}
U_{j+1/2}^{n+1} =& \frac{1}{2}(U_j^n + U_{j+1}^n) + \frac{1}{8}\big[(U_j^n)' - (U_{j+1}^n)'\big] \\
&+ \frac{1}{\Delta x}\int_n^{n+1} F\big(U(x_j,),V(x_j,)\big) - F\big(U(x_{j+1},),V(x_{j+1},)\big)\,dt, \\
V_{j+1/2}^{n+1} =& \frac{1}{2}(V_j^n + V_{j+1}^n) + \frac{1}{8}\big[(V_j^n)' - (V_{j+1}^n)'\big] \\
&+ \frac{1}{\Delta x}\int_n^{n+1}\int_{x_j}^{x_{j+1}} G\big(U(x,),V(x,),U_x(x,),V_x(x,)\big)\,dx\,dt.
\end{aligned}$$

The semi-discrete approximation can be rewritten in the form

$$U_{j+1/2}^{n+1} = \frac{1}{2}(U_j^n + U_{j+1}^n) - \frac{1}{8}\big[(U_{j+1}^n)' - (U_j^n)'\big] - \lambda(F_{j+1} - F_j), \tag{71}$$

$$V_{j+1/2}^{n+1} = \frac{1}{2}(V_j^n + V_{j+1}^n) - \frac{1}{8}\big[(V_{j+1})' - (V_j^n)'\big] - \Delta\, G_{j+1/2}, \tag{72}$$

where $\lambda = \Delta/\Delta x$ and

$$F_j = \frac{1}{\Delta}\int_n^{n+1} F\big(U(x_j,),V(x_j,)\big)\,dt, \tag{73}$$

$$G_{j+1/2} = \frac{1}{\Delta}\int_n^{n+1}\frac{1}{\Delta x}\int_{x_j}^{x_{j+1}} G\big(U(x,),V(x,),U_x(x,),V_x(x,)\big)\,dx\,dt. \tag{74}$$

To achieve the second order accuracy in space for smooth solutions we use a midpoint rule to approximate the space integral in (74) and then apply central differencing to the space derivatives to get

$$\begin{aligned}
&\frac{1}{\Delta x}\int_{x_j}^{x_{j+1}} G\big(U(x,),V(x,),U_x(x,),V_x(x,)\big)\,dx \\
\approx& G\big(U(x_{j+1/2},),V(x_{j+1/2},),U_x(x_{j+1/2},),V_x(x_{j+1/2},)\big) \\
\approx& G\Big(U(x_{j+1/2},),V(x_{j+1/2},),\frac{U(x_{j+1},)-U(x_j,)}{\Delta x},\frac{V(x_{j+1},)-V(x_j,)}{\Delta x}\Big).
\end{aligned} \tag{75}$$

To guarantee the non-oscillatory nature of the scheme we use the non-oscillatory TVD numerical derivative for U and V

$$U_j' = \text{Minmod}\,(\Delta \mathrm{U_{j+1/2}},\, \Delta \mathrm{U_{j-1/2}}), \tag{76}$$

$$V_j' = \text{Minmod}\,(\Delta \mathrm{V_{j+1/2}},\, \Delta \mathrm{V_{j-1/2}}), \tag{77}$$

where $\Delta U_{j+1/2} = u_{j+1} - u_j$, $\Delta V_{j+1/2} = V_{j+1} - V_j$ and Minmod is the multivariable MinMod function given by

$$\text{Minmod}\,(\mathrm{x_1}, \mathrm{x_2}, \cdots) = \begin{cases} \min\limits_j\{x_j\} & \text{if } \ x_j > 0, \ \ \forall\, j, \\ \max\limits_j\{x_j\} & \text{if } \ x_j < 0, \ \ \forall\, j, \\ 0 & \text{otherwise.} \end{cases} \tag{78}$$

However other choices, like UNO numerical derivatives are also possible (cf. [14, 27]).

4.2.1 Semi-implicit Predictor-Corrector Time Discretization

To define the numerical scheme we should approximate the time integrals

$$\frac{1}{\Delta}\int_n^{n+1} F\big(U(x_j,),V(x_j,)\big)\,dt, \tag{79}$$

$$\frac{1}{\Delta}\int_n^{n+1} G\Big(U(x_{j+1/2},),V(x_{j+1/2},),\frac{U(x_{j+1},)-U(x_j,)}{\Delta x},\frac{V(x_{j+1},)-V(x_j,)}{\Delta x}\Big). \tag{80}$$

This can be done in different ways, and we refer [28, 29] for a recent discussion on several second order time discretizations for hyperbolic systems with relaxation. Stability considerations suggest the use of implicit time integrators for the previous system (79)–(80). From our numerical experiments this seems essential in the computation of high Mach number flows. For example a backward Euler type method is given by

$$\frac{1}{\Delta}\int_n^{n+1} F\big(U(x_j,),V(x_j,)\big)\,dt \approx F\big(U(x_j,^{n+1}),V(x_j,^{n+1})\big), \tag{81}$$

$$\begin{aligned}&\frac{1}{\Delta}\int_n^{n+1} G\Big(U(x_{j+1/2},),V(x_{j+1/2},),\frac{U(x_{j+1},)-U(x_j,)}{\Delta x},\frac{V(x_{j+1},)-V(x_j,)}{\Delta x}\Big)\\ \approx& G\Big(U^{n+1}_{j+1/2},V^{n+1}_{j+1/2},\frac{U(x_{j+1},^{n+1})-U(x_j,^{n+1})}{\Delta x},\frac{V(x_{j+1},^{n+1})-V(x_j,^{n+1})}{\Delta x}\Big),\end{aligned} \tag{82}$$

where the values of $U(x_j,^{n+1})$ and $V(x_j,^{n+1})$ must be computed using a suitable predictor formula. We use the explicit approximations

$$U(x_j,^{n+1})\approx U_j^{n+1}=U_j^n+\lambda(F_j^n)', \tag{83}$$

$$V(x_j,^{n+1})\approx V_j^{n+1}=V_j^n+\Delta\, G\Big(U_j^{n+1},V_j^{n+1},\frac{(U_j^n)'}{\Delta x},\frac{(V_j^n)'}{\Delta x}\Big), \tag{84}$$

where $(F_j^n)'/\Delta x$ is at least a first order approximation of $F\big(U(x_j,^n),V(x_j,^n)\big)_x$, computed for example using the same MinMod limiter. Thanks to the explicit predictor and the linear nature of G with respect to V_j^{n+1} this scheme under development can be implemented explicitly.

Remark 4.1. *Note that slightly better stability properties without increasing the computational complexity of the algorithm can be obtained by taking U_j' also at time $^{n+1}$ instead of ^{n} in the predictor step (84). Alternatively a fully implicit approach will require the use of some iterative solvers in the predictor step.*

Collecting all together (73)–(75) and (81)–(82) we have the numerical scheme given by the predictor (83)–(84) and the corrector

$$U^{n+1}_{j+1/2}=\frac{1}{2}(U_j^n+U_{j+1}^n)-\frac{1}{8}\big[(U_{j+1}^n)'-(U_j^n)'\big]-\lambda\big(F(U_{j+1}^{n+1},V_{j+1}^{n+1})-F(U_j^{n+1},V_j^{n+1})\big), \tag{85}$$

$$V^{n+1}_{j+1/2}=\frac{1}{2}(V_j^n+V_{j+1}^n)-\frac{1}{8}\big[(V_{j+1}^n)'-(V_j^n)'\big] \tag{86}$$

$$-\Delta t G\Big(U^{n+1}_{j+1/2},V^{n+1}_{j+1/2},\frac{U_{j+1}^{n+1}-U_j^{n+1}}{\Delta x},\frac{V_{j+1}^{n+1}-V_j^{n+1}}{\Delta x}\Big), \tag{87}$$

where U_j^{n+1} and V_j^{n+1} on the right hand side are given by (83) and (84). Although the above scheme has some implicit terms, it can be solved explicitly by first obtaining $U^{n+1}_{j+1/2}$ and then use it in (87), since G is linear in V and V_x.

Remark 4.2. *To obtain second order accuracy in time for moderate stiff problems it is enough to replace the time integrations in (81) and (82) by the trapezoidal rule. The construction of*

time discretizations that work with uniform second order accuracy with respect to the stiffness parameter is currently under investigations.

Remark 4.3. *Different strategies may also be adopted to remove the staggering from the grid. For example using a nonstaggered high resolution Lax-Friedrichs scheme as in [27] or simply using a projection technique like in [15]. This will be particularly important in consideration of future multidimensional computations.*

4.2.2 Diffusive Terms

Finally, the system containing diffusive and source terms

$$U_{=}0, \qquad V_{=}D(U,V,U_x,V_x)_x, \tag{88}$$

are approximated by standard central difference on the grid point x_j in the form

$$\begin{aligned} & D(U,V,U_x,V_x)_x\,|_{x=x_j} \\ \approx & \frac{1}{\Delta x}\left[D\Big(U_{j+1/2},V_{j+1/2},\frac{U_{j+1}-U_j}{\Delta x},\frac{V_{j+1}-V_j}{\Delta x}\Big)\right. \\ & \left. - D\Big(U_{j-1/2},V_{j-1/2},\frac{U_j-U_{j-1}}{\Delta x},\frac{V_j-V_{j-1}}{\Delta x}\Big)\right], \end{aligned}$$

combined with a fully implicit backward Euler discretization in time. For the approximation of the values $U_{j\pm1/2}$ and $V_{j\pm1/2}$ we use the simple averages

$$U_{j\pm1/2}=\frac{U_j+U_{j\pm1}}{2}, \qquad V_{j\pm1/2}=\frac{V_j+V_{j\pm1}}{2}.$$

The resulting discretization forms a tridiagonal linear system that can be solved efficiently in a direct way. The same clearly applies if we consider its natural second order extension based on the Crank-Nicolson time integration.

Remark 4.4. *The combination of the two steps (62) and (63) gives a first order splitting scheme in time. Second order extensions can be obtained using Strang splitting*[35] *or the Runge-Kutta schemes presented in [2, 29].*

5 Numerical Results

In this section we compare numerical solutions of the one dimensional stationary shock waves for rarefied gas dynamics obtained by the Relaxed-Burnett (RB) equations (40)–(45), the Navier-Stokes equations and the Extended Thermodynamics (ET) approximations. Serving as reference solutions we use the results given by Monte Carlo simulations (DSMC) for the full Boltzmann equation.

The DSMC simulations have been performed in the case of Maxwellian molecules and thanks to the stationary nature of the problem an efficient averaging technique has been used to obtain profiles with a small amount of fluctuations. We refer to [3, 30] for further details.

For the sake of completeness we present also the the Navier-Stokes (NS) equations

$$\begin{aligned} & \rho_+(\rho u)_x=0, \qquad (\rho u)_+(\rho u^2+p+\sigma)_x=0, \\ & \Big(\frac{1}{2}\rho u^2+\frac{3}{2}p\Big)_+\Big(\frac{1}{2}\rho u^3+\frac{5}{2}up+\sigma u+q\Big)_x=0, \\ & \sigma=-\frac{4}{3}\mu u_x, \qquad q=-\frac{3}{2}\mu\mathcal{M}R\,\theta_x, \qquad \mu=\epsilon\theta, \end{aligned} \tag{89}$$

and the Extended Thermodynamics (ET) equations

$$\begin{aligned}
&\rho_+(\rho u)_x = 0, \qquad (\rho u)_+(\rho u^2 + p + \sigma)_x = 0,\\
&\Big(\frac{1}{2}\rho u^2 + \frac{3}{2}p\Big)_+\Big(\frac{1}{2}\rho u^3 + \frac{5}{2}up + \sigma u + q\Big)_x = 0,\\
&\Big(\frac{2}{3}\rho u^2 + \sigma\Big)_+\Big(\frac{2}{3}\rho u^3 + \frac{4}{3}up + \frac{7}{3}\sigma u + \frac{8}{15}q\Big)_x = -\frac{\rho\sigma}{\epsilon},\\
&(\rho u^3 + 5up + 2\sigma u + 2q)_+\Big(\rho u^4 + 5\frac{p^2}{\rho} + 7\frac{\sigma p}{\rho} + \frac{32}{5}qu + u^2(8p + 5\sigma)\Big)_x = -\frac{2\rho}{\varepsilon}\Big(\frac{2}{3}q + \sigma u\Big).
\end{aligned} \tag{90}$$

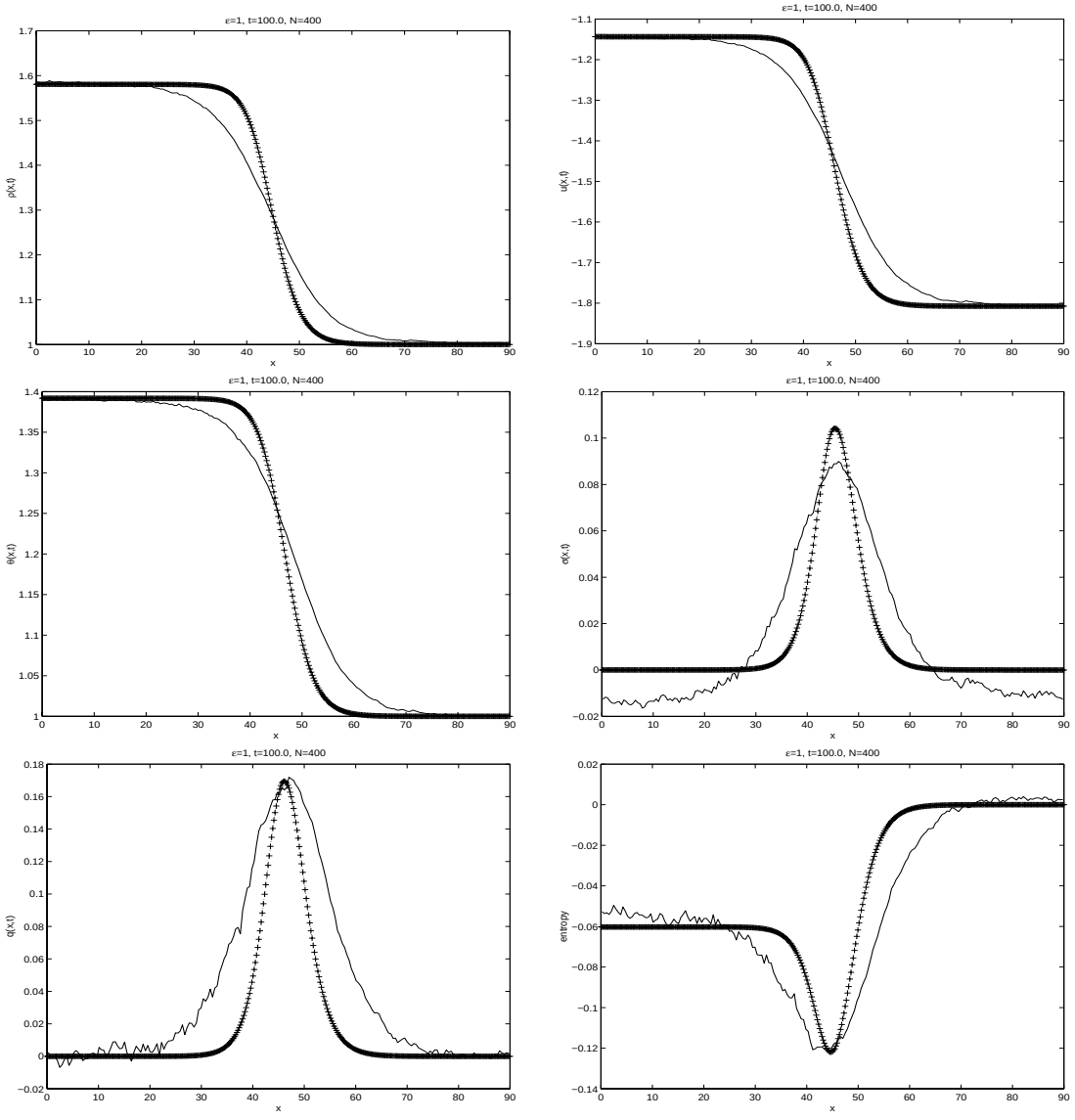

Fig. 1(a) Numerical solution of Navier-Stokes equations for M=1.4 at time =100. Continuous line DSMC result.

Note that the ET equations, with the number of moments used in (90), are the same as Grad's thirteen moment equations[26].

Both system has been solved using the same staggered grid. For system (89) we have adapted the same discretization as for the RB system (by removing all the Burnett and super Burnett orders). While for system (90) we use the central scheme recently proposed in [28]. We omit the details.

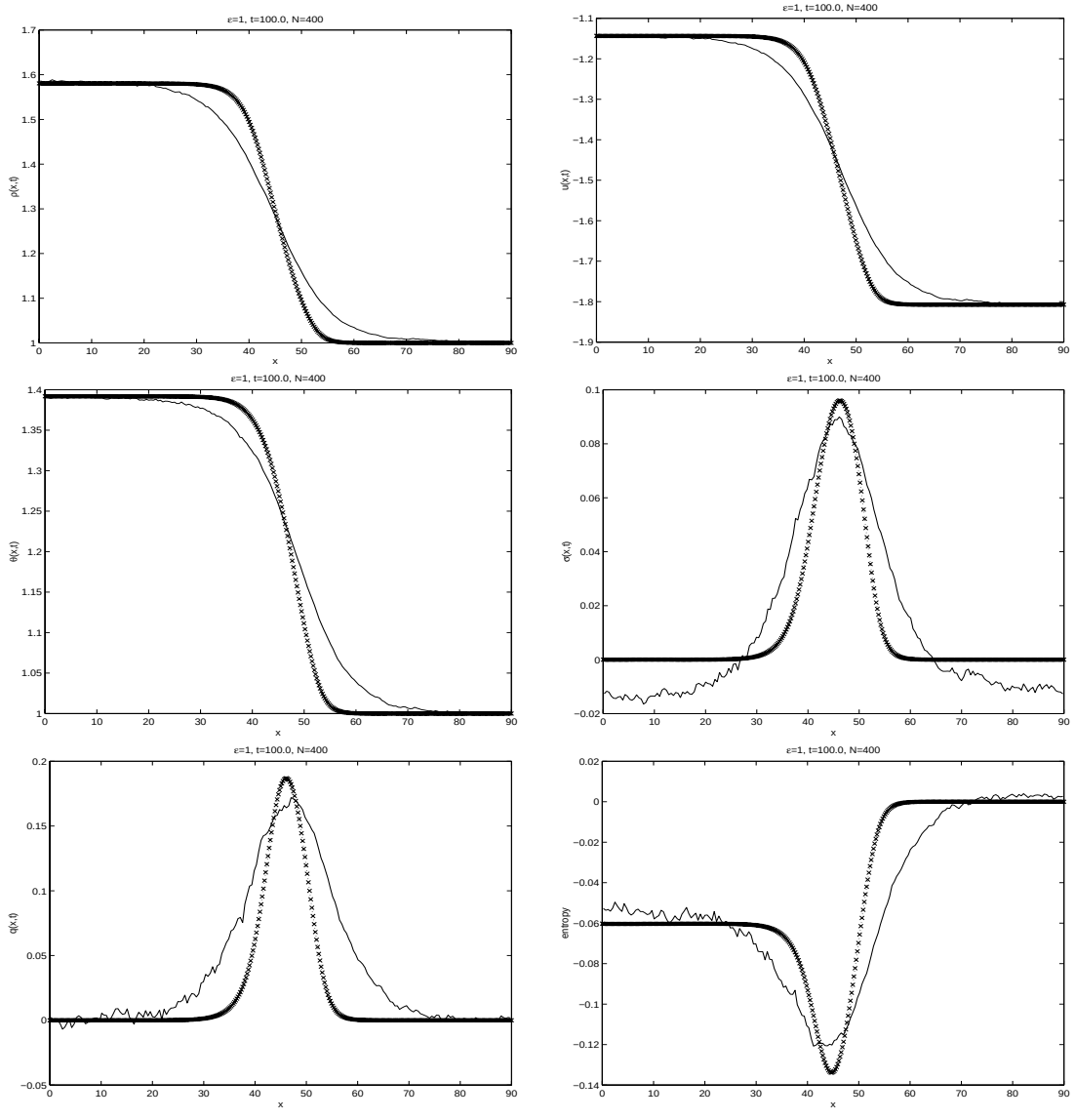

Fig. 1(b) Numerical solution of Extended-Thermodynamics equations for M=1.4 at time =100. Continuous line DSMC result.

The relaxation model has been considered in the form (56) with $\mu = \varepsilon\,\theta$ (Maxwellian molecules), $R = 1$ and the set of parameters given by (18).

The test problem is given by a one-dimensional stationary shock profiles for $\varepsilon = 1$ and different values of the Mach number ranging form 1.4 to 10. In all our numerical examples the gas is initially at the upstream equilibrium state in the left half-space and in the downstream equilibrium state in the right-half space. The two states being smoothly connected with an

hyperbolic tangent function.

The upstream state is determined from the downstream state using the Rankine-Hugoniot relations [37].

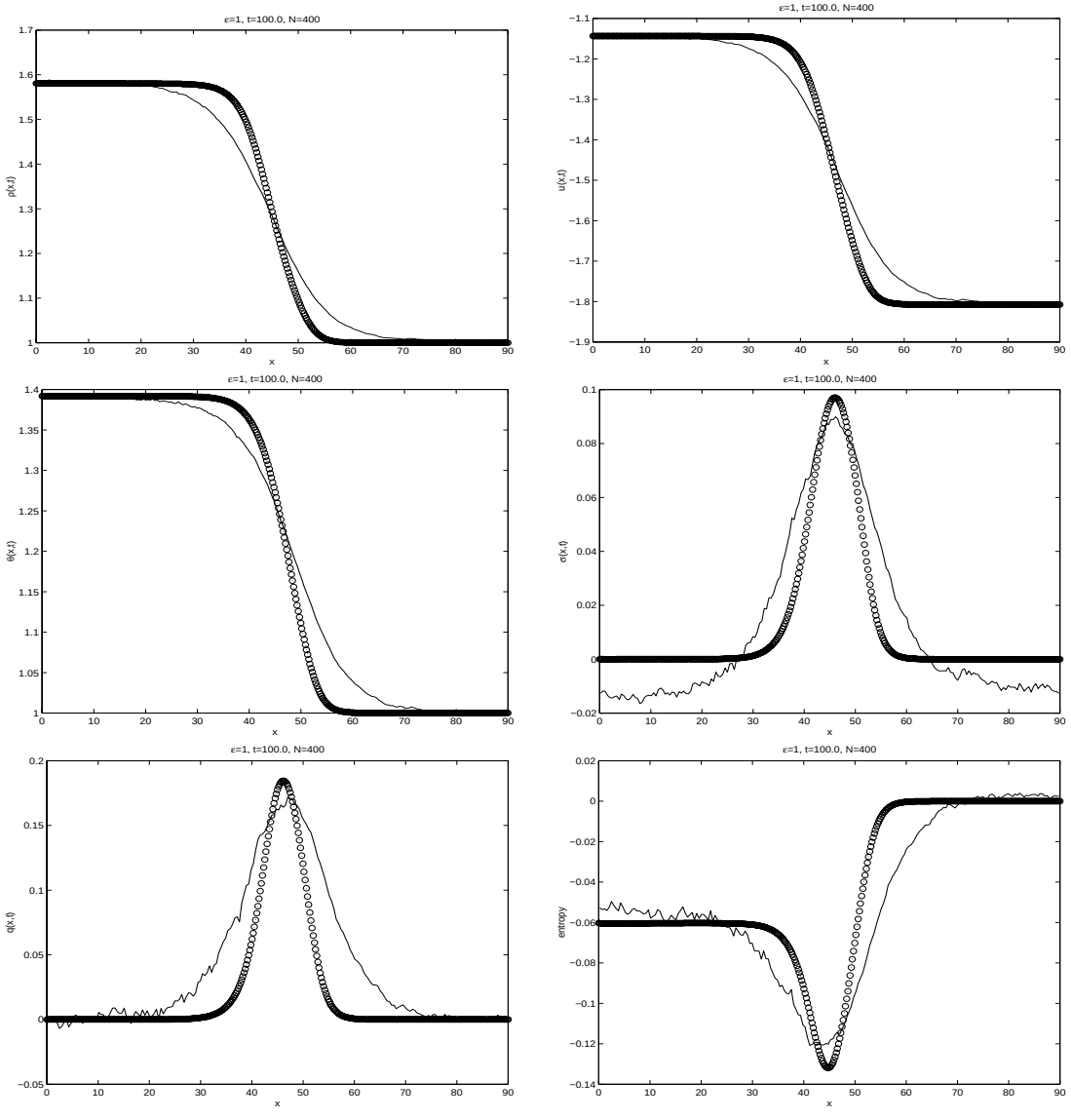

Fig. 1(c) Numerical solution of Relaxed-Burnett equations for M=1.4 at time =100. Continuous line DSMC result.

In the present calculations, the downstream state is characterized by $\rho = 1.0$, $T = 1.0$, and by the Mach number M of the shock. The downstream mean velocity is then given by $u = -M\sqrt{\gamma T}$, with $\gamma = 5/3$.

The infinite physical space is truncated to the finite region $[-L, L]$ where L depends on the Mach number considered. The reference solution is obtained using the DSMC method with 200 space cells and 100 particles in each downstream cell and averaging over approximatively 10^6 time steps after the 'stationary time' = 100. We report the result obtained with the different

schemes using 400 space cells at time = 100 after the stationary state has been reached.

We remark that the relaxed Burnett equations (56) have the additional free parameters $\widehat{\theta}_2, \widehat{\theta}_3, \widehat{\theta}_4$ and $\widehat{\omega}_2, \widehat{\omega}_3, \widehat{\omega}_4$ at the super Burnett terms. A possible strategy to select these parameters is to perform a least square fitting procedure on several test cases with different Mach numbers. Our results suggest that these values can be chosen independently of the Mach number and that a reasonable choice, based on the least square fitting of a Mach 4 shock obtained by the DSMC, is given by

$$\widehat{\theta}_2 = -60, \quad \widehat{\theta}_3 = 100, \quad \widehat{\theta}_4 = 25, \qquad \widehat{\omega}_2 = -20, \quad \widehat{\omega}_3 = 20, \quad \widehat{\omega}_4 = 20.$$

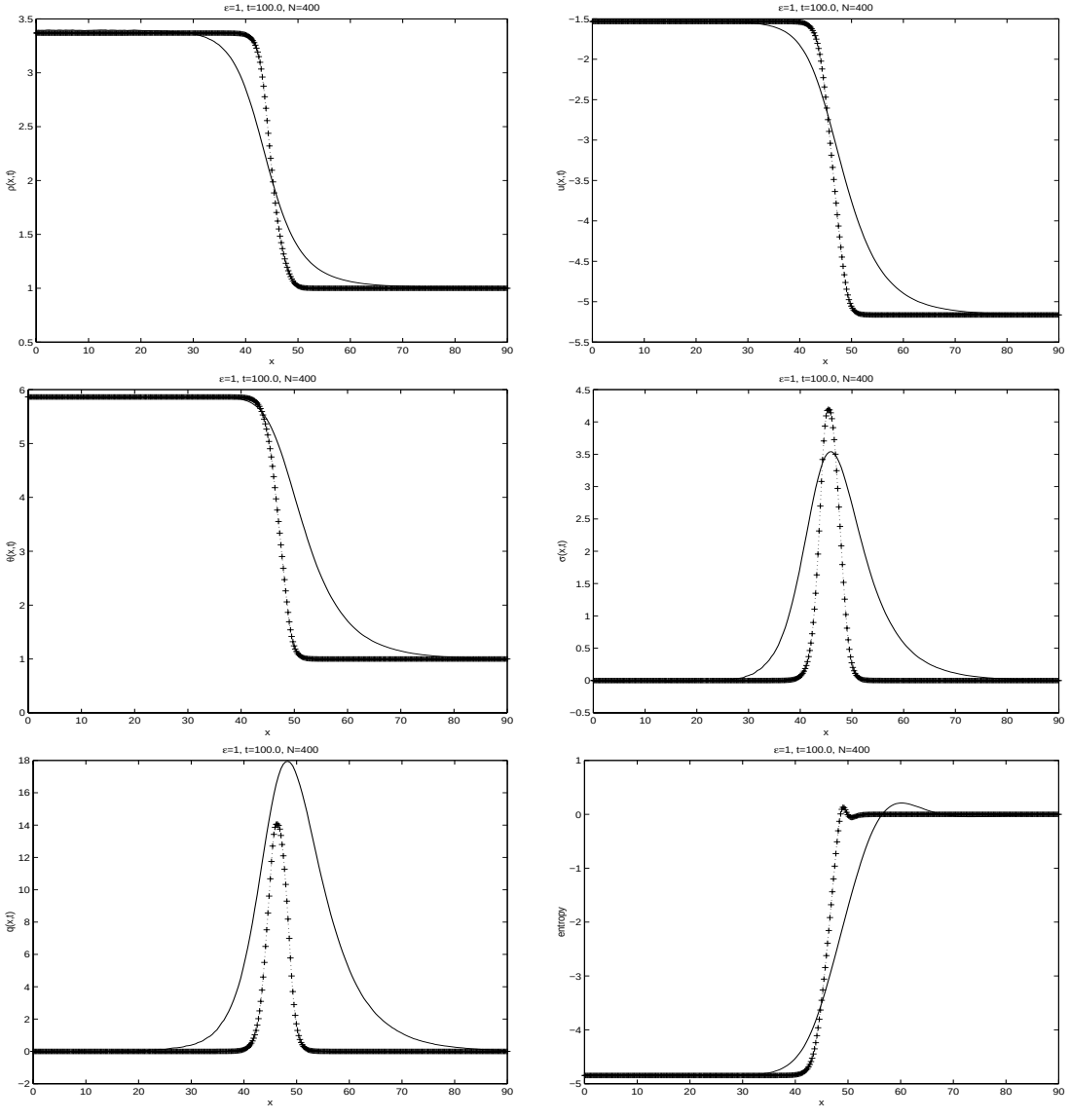

Fig. 2(a) Numerical solution of Navier-Stokes equations for M=4.0 at time =100. Continuous line DSMC result.

Unfortunately this set of parameters does not satisfy the sufficient condition for a generalized entropy inequality stated by Theorem 3.1 (since $\widehat{\omega}_2$, $\widehat{\omega}_3$ and $\widehat{\theta}_3$ are positive). However numerical

evidence seems to indicate that the same entropy inequality holds. It is an open question to understand if it is possible to remove some of the sign assumptions in the proof.

The entropy function

$$\eta = \log(\rho) - \frac{3}{2}\log(\theta) + \frac{\omega_2(p_{11}-p)^2}{8p^2} + \frac{2\theta_2 q^2}{9\mathcal{M}^2\rho^2\theta^3}. \tag{91}$$

has been computed for all models (including DSMC).

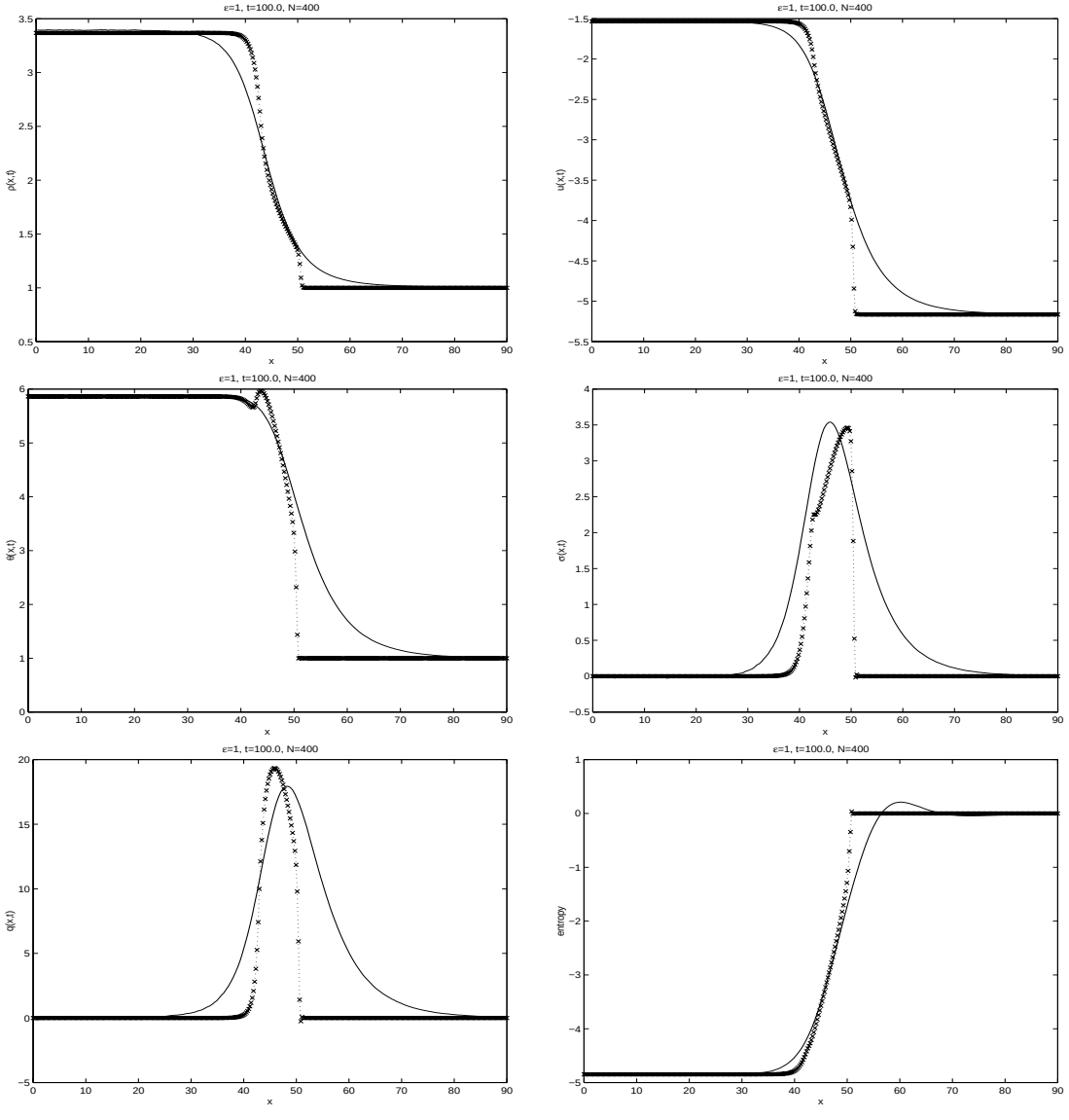

Fig. 2(b) Numerical solution of Extended-Thermodynamics equations for M=4.0 at time =100. Continuous line DSMC result.

In Figures 1(a,b,c), we plot the result obtained for $M = 1.4$ using the different models. The convergence speed to the stationary state is comparable. As expected, the results show that essentially all approximations are almost equivalent and provide a reasonable good description of the rarefied shock. The same conclusions can be drawn for weaker shocks where the Mach

number is closer to one.

Next we consider the case of $M = 4.0$ (see Figures 2(a,b,c)). A marked improvement of the numerical solution obtained with the RB model with respect to ET and NS models is evident in the computations of all physical quantities. A slightly more restrictive CFL condition is required by the RB central scheme if compared with the corresponding ET and NS central schemes (about one half).

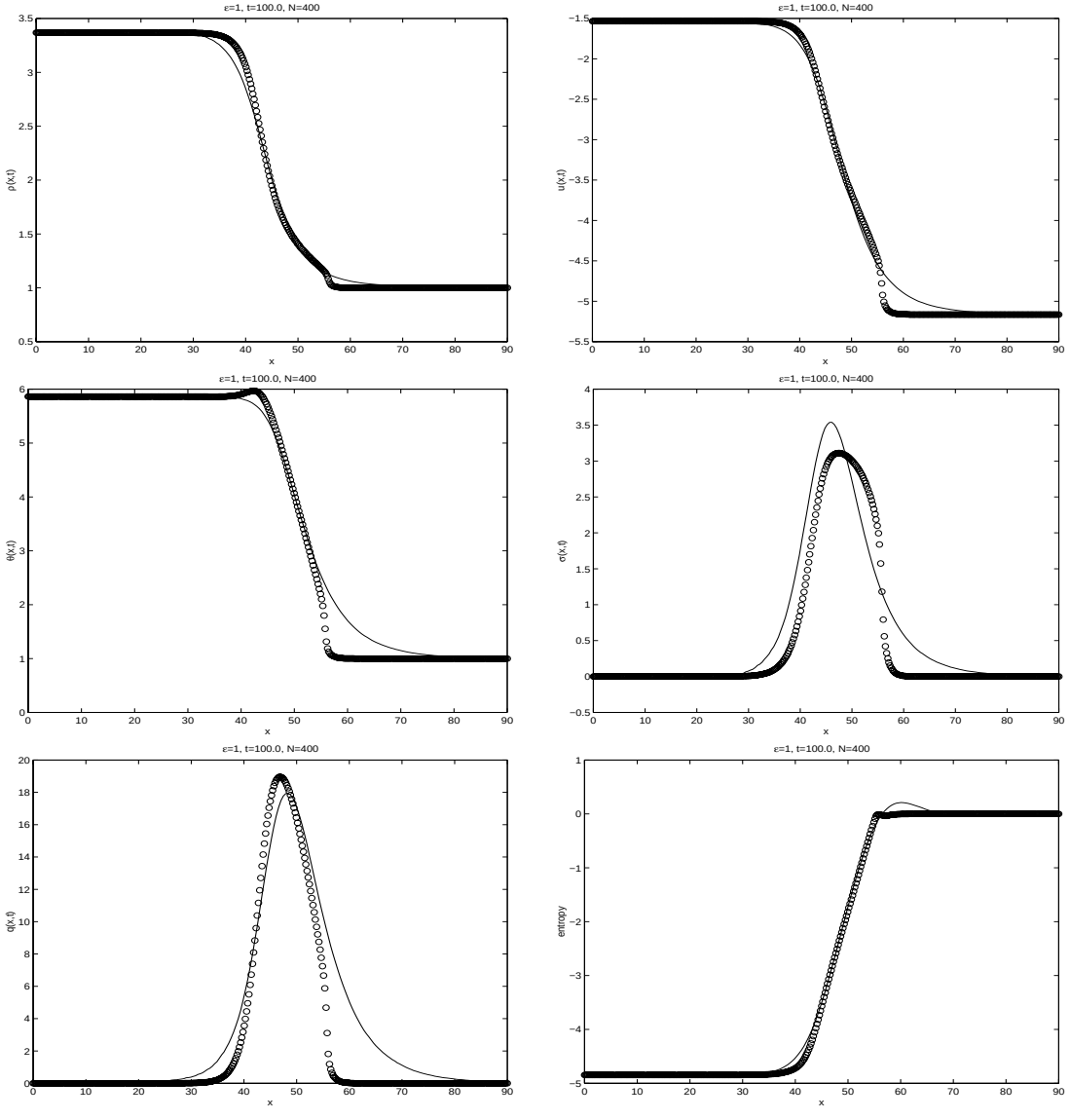

Fig. 2(c) Numerical solution of Relaxed-Burnett equations for M=4.0 at time =100. Continuous line DSMC result.

Finally we give the result of the computations for $M = 10$ in Figures 3(a,b,c). Again the solution obtained with the RB equations outperforms the solutions of the ET and NS equations. However the restriction on the CFL condition of the RB scheme here is more severe and it is an open question at present to understand if this is due to an increase of stiffness with the Mach

number in the RB equations or to some instability phenomena that occur in the RB model at very high Mach numbers. This is under study.

6 Conclusions

We have proposed a class of relaxation schemes for the one-dimensional Boltzmann equation based on the relaxed Burnett system by Jin and Slemrod[16]. The schemes combine a conservative solver for the conserved part of the system (balance laws for density, momentum and energy), while for the equations in non conservative form (heat flux and stress) we discretize the spatial derivatives using slope limiters and central differences. This is carried out conveniently using a staggered grid, as in a staggered non-oscillatory central scheme (cf. [27]).

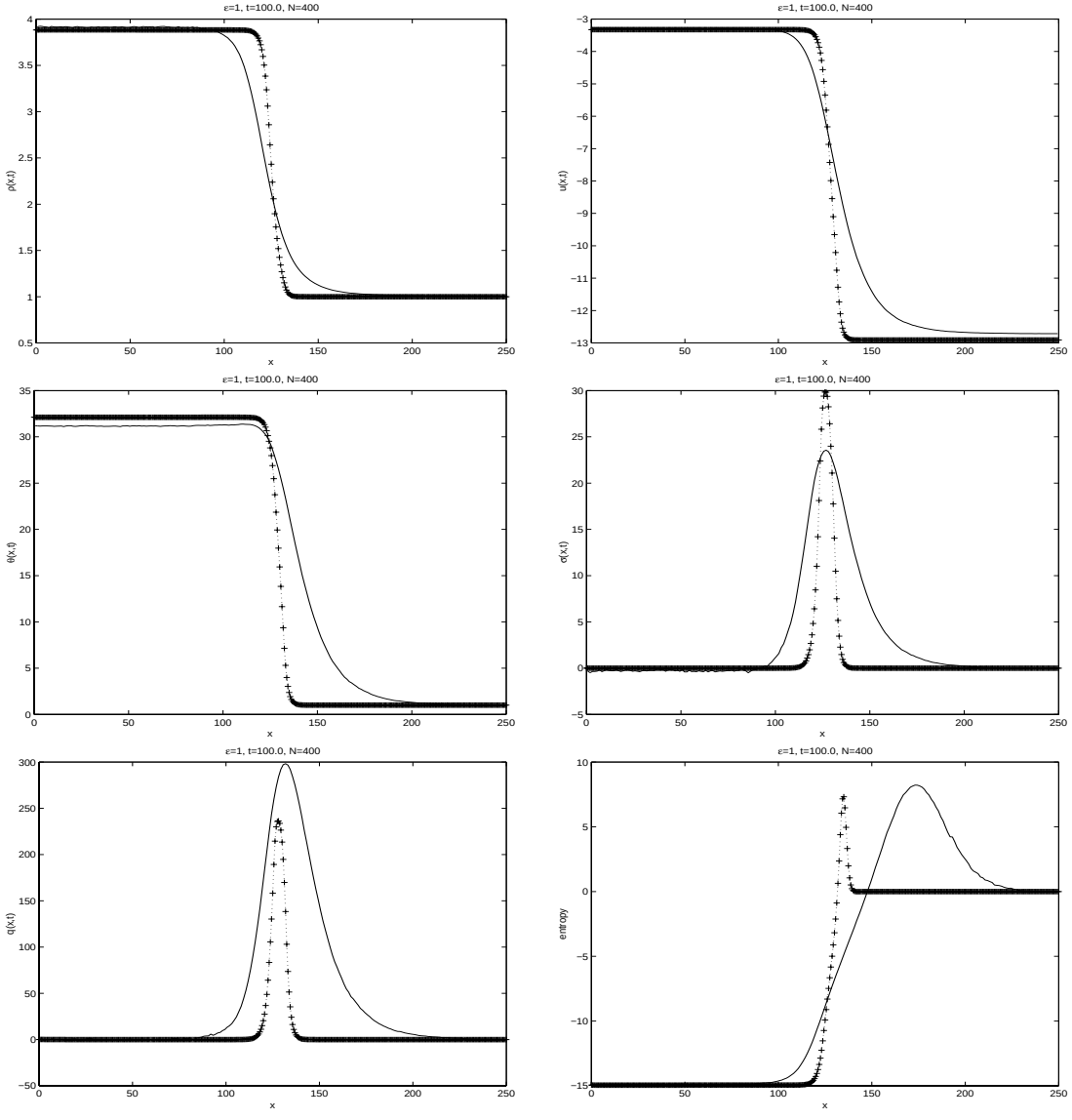

Fig. 3(a) Numerical solution of Navier-Stokes equations for M=10.0 at time =100. Continuous line DSMC result.

The numerical results for a stationary shock wave with different Mach numbers are promising and it appears that the relaxed Burnett system offers more accurate shock profiles compared to the DSMC than other hydrodynamic theories (Navier-Stokes and extended thermodynamics). Further numerical experiments and extension of the present schemes to the multi-dimensional case will be presented elsewhere.

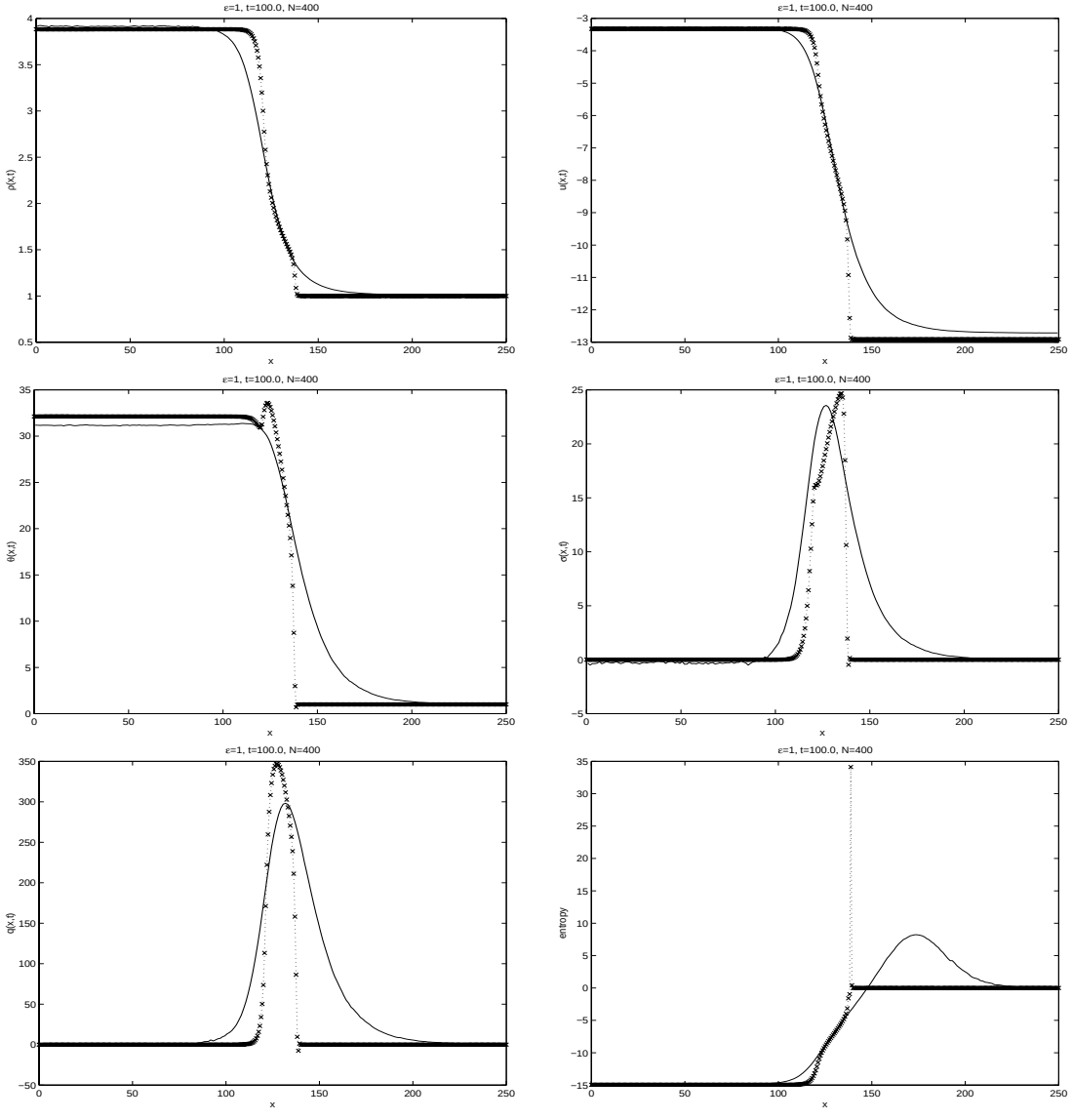

Fig. 3(b) Numerical solution of Extended-Thermodynamics equations for M=10.0 at time =100. Continuous line DSMC result.

Nomenclature

b body force
$\mathcal{B}$ subset of Euclidean space
div divergence
e internal energy density

grad gradient
$\boldsymbol{I}$ unit tensor
$\boldsymbol{L}$ velocity gradient $(\boldsymbol{L} = \mathrm{grad}\,\boldsymbol{u})$
$\mathcal{M}$ Maxwell number
$\boldsymbol{n}$ unit exterior normal
$\boldsymbol{P}$ pressure deviator $(\boldsymbol{P} = [P^{ij}]_{3\times 3})$
$\boldsymbol{p}$ mean normal pressure

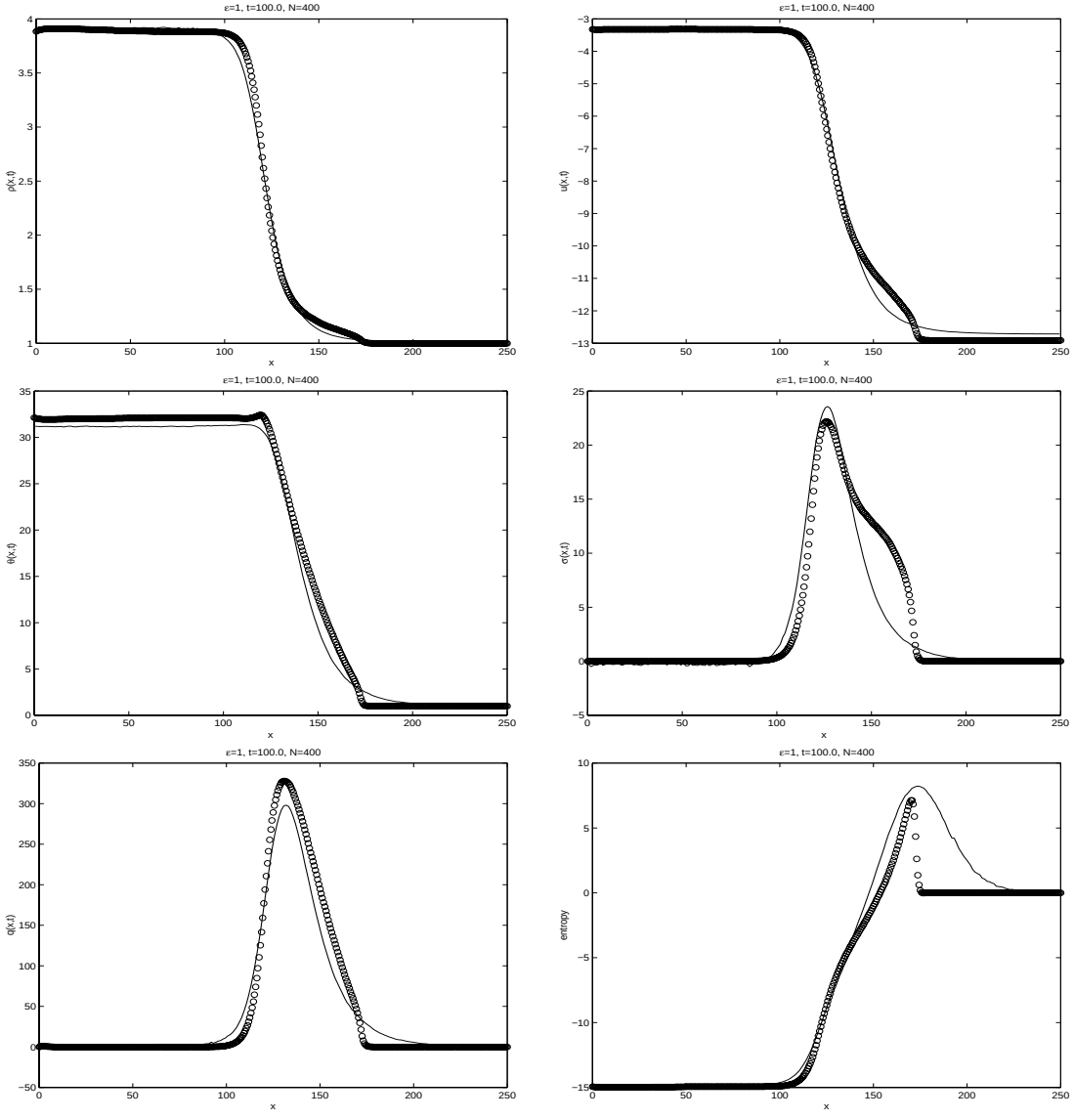

Fig. 3(c) Numerical solution of Relaxed-Burnett equations for M=10.0 at time =100. Continuous line DSMC result.

$\boldsymbol{q}$ energy flux vector $(\boldsymbol{q} = [q_1, q_2, q_3]^T)$
$\boldsymbol{R}$ gas constant
$\boldsymbol{S}$ distortion tensor $\left(\boldsymbol{S} = \frac{1}{2}(\mathrm{grad}\,\boldsymbol{u} + (\mathrm{grad}\,\boldsymbol{u})^T - \frac{2}{3}\,\mathrm{div}\,\boldsymbol{u}\boldsymbol{I})\right)$

$\boldsymbol{T}$ stress tensor ($\boldsymbol{T} = -p\boldsymbol{I} - \boldsymbol{P}$)
$\boldsymbol{t}$ time
$\mathbf{tr}$ trace
$\boldsymbol{u}$ macroscopic velocity
$\boldsymbol{x}$ cartesian coordinate $\big(\boldsymbol{x} = (x, y, z)\big)$
μ viscosity
ρ mass density
η specific entropy
ψ Helmhotz free energy, $\psi = \varepsilon - \theta\eta$
θ temperature
θ_i, $\widehat{\theta}_i$ coefficients of the Chapman-Enskog expansion for $\boldsymbol{q}$
ω_i, $\widehat{\omega}_i$ coefficients of the Chapman-Enskog expansion for $\boldsymbol{P}$
$\widehat{\gamma}_1$, $\widehat{\lambda}_1$ coefficients of the super Burnett terms
$(^\bullet)$ material derivative of ( ), i.e. $(^\bullet) = \frac{\partial}{\partial}( ) + \boldsymbol{u} \cdot$ grad ( )
$\otimes$ dyadic product, i.e. $(\boldsymbol{u} \otimes \boldsymbol{v})_{ij} = u_i v_j$
$\cdot$ inner product, i.e. $\boldsymbol{u} \cdot \boldsymbol{v} = u_i v_i$ for vectors $\boldsymbol{u}, \boldsymbol{v}$;
$\boldsymbol{A} \cdot \boldsymbol{B} = \mathrm{tr}(\boldsymbol{A}B)$ for tensors $\boldsymbol{A}, \boldsymbol{B}$.

Acknowledgement L. Pareschi thanks the Department of Mathematics and Center for the Mathematical Sciences at University of Wisconsin-Madison for their hospitality during his visit.

References

[1] Agarwal, R., Yun, K., Balakrishnan, R. Beyond Navier-Stokes: Burnett Equations for Flow Simulations in Continuum-transition Regime. AIAA 99-3580, 30th AIAA Fluid Dynamics Conference, Norfolk, VA, 28 June–1 July, 1999
[2] Ascher, U., Ruth, S., Spiteri, R.J. Implicit-explicit Runge-Kutta Methods for Time Dependent PDE's. *Appl. Numer. Math.*, 1997, 25: 151–161
[3] Bird, G.A. Molecular Gas Dynamics. Oxford University Press, London, 1994
[4] Biscari, P., Cercignani, C., Slemrod, M. Time Derivatives and Frame Indifference Beyond Newtonian Fluids. *C.R. Acad. Sci. Paris* (Series 11), 2000, 328(b): 417–422
[5] Bobylev, A.V. The Chapman-Enskog and Grad Methods for Solving the Boltzmann Equation. *Soviet Physics Doklady*, 1982, 27(1): 71–75
[6] Bobylev, A.V. On the Structure of Spatially Homogeneous Normal Solutions of a Nonlinear Boltzmann Equation for a Mixture of Gases. *Soviet Physics Doklady*, 1980, 25: 30–32
[7] Cercignani, C. The Boltzmann Equation and Its Applications. Springer-Verlag, New York, 1988
[8] Chen, G.Q., Levermore, C.D., Liu, T.P. Hyperbolic Conservation Laws with Stiff Relaxation Terms and Entropy. *Communications in Pure and Applied Mathematics*, 1994, 47: 787–830
[9] Coquel, F., Perthame, B. Relaxation of Energy and Approximate Riemann Solvers for General Pressure Laws in Fluid Dynamics. *SIAM J. Num. Anal.*, 1998, 35: 2223–2249
[10] Ferziger, J.H., Kaper, H.G. Mathematical Theory of Transport Processes in Gases. North Holland, Amsterdam, 1972
[11] Fiscko, K.A., Chapman, D.R. Comparison of Burnett, Super-Burnett and Monte-Carlo Solutions for Hypersonic Shock Structure. Proc.16th International Symposium on Rarefied Gas Dynamics, Pasadena, California, July 11–15, 1988
[12] Foch, T.D. On the Higher Order Hydrodynamic Theories of Shock Structure. *Acta Physica Austriaca, Supplement*, 1973, **X**: 123–140
[13] Grad, H. Asymptotic Theory of the Boltzmann Equation. *Physics of Fluids*, 1963, 6: 147–181
[14] Harten, A., Osher, S. Uniformly High Order Accurate Non-oscillatory Scheme I. *SIAM J. Numer. Anal.*, 1987, 24: 279–309
[15] Jang, G.S., Levy, D., Lin, C.T., Osher, S., Tadmor, E. High-resolution Non-oscillatory Central Schemes with Non-staggered Grids for Hyperbolic Conservation Laws. *SIAM J. Num. Anal.*, 1998, 35: 1892–1917
[16] Jin, S., Slemrod, M. Regularization of the Burnett Equations via relaxation. *J. Stat. Phys.*, 2001, 103(5-6): 1009–1033
[17] Jin, S., Slemrod, M. Regularization of the Burnett Equations for Fast Granular Flows via Relaxation. *Physica D*, 2001, 150: 207–218
[18] Jin, S., Xin, Z.P. The Relaxation Schemes for Systems of Conservation Laws in Arbitrary Space Dimensions. *Comm. Pure Appl. Math.*, 1995, 48: 235–276

[19] Joseph, D.D. Fluid Dynamics of Viscoelastic Liquids. Springer-Verlag, New York, 1990
[20] Levermore, C.D. Moment Closure Hierarchies for Kinetic Theories. *J. Stat. Phys.*, 1996, 83: 1021–1065
[21] Levermore, C.D., Morokoff, W.J. The Gaussian Moment Closure for Gas Dynamics. *SIAM J. Appl. Math.*, 1998, 59: 72–96
[22] Liotta, F., Romano, V., Russo, G. Central Schemes for Balance Laws of Relaxation Type. *SIAM J. Numer. Anal.*, 2000, 38: 1337–1356
[23] Luk'shin, A.V. On the Method of Derivation of Closed Systems for Macroparameters of Distribution Function for Small Knudsen Numbers. *Doklady AN SSSR* , 1983, 170: 869–873 English Translation in *Soviet Physics Doklady*, 1983, 28: 454–456
[24] Luk'shin, A.V. Hydrodynamical Limit for the Boltzmann Equation and Its Different Analogs. In: Numerical and Analytical Methods in Rarefied Gas Dynamics, Moscow Aviation Institute, Moscow 1986, 37–43
[25] Luk'shin, A.V. The Cauchy Problem for the Boltzmann Equation. Hydrodynamical limit. In: Numerical Methods in Mathematical Physics, Moscow State University, Moscow 1986, 61–91
[26] Müller, I., Ruggeri, T. Rational Extended Thermodynamics. 2nd ed., Springer, 1998
[27] Nessyahu, H., Tadmor, E. Nonoscillatory Central Differencing for Hyperbolic Conservation Laws. *J. Comp. Phys.*, 1990, 87: 408–463
[28] Pareschi, L. Central Differencing Based Numerical Schemes for Hyperbolic Conservation Laws with Relaxation Terms. *SIAM J. Num. Anal.*, 2001, 39(4): 1395–1417
[29] Pareschi, L., Russo, G. Implicit-Explicit (IMEX) Runge-Kutta Schemes for Stiff Systems of Differential Equations. *Advances in Theor. of Comp. Math.*, Vol.3, Recent Trends in Numerical Analysis, Donato Trigiante Ed., 269–288, 2000
[30] Pareschi, L., Russo, G. An Introduction to Monte Carlo Methods for the Boltzmann Equation. ESAIM: Proceedings, CEMRACS 1999, Vol.10, 35–75, 2001
[31] Renardy, M. On the Domain Space for Constitutive Laws in Linear Viscoelasticity. *Arch. Rat. Mech. Anal.*, 1984, 85: 21–26
[32] Sanders, R., Weiser, A. A High Order Staggered Grid Method for Hyperbolic Systems of Conservation Laws in One Space Dimension. *Comp. Meth. in App. Mech. an Engrg.*, 1989, 75: 91–107
[33] Slemrod, M. Constitutive Relations for Monatomic Gases Based on a Generalized Rational Approximation to the Sum of the Chapman-Enskog Expansion. To Appear, *Arch. Rational Mech. Anal.*, 1999, 150(1): 1–22
[34] Slemrod, M. In the Chapman-Enskog Expansion the Burnett Coefficients Satisfy the Universal Relation $\Omega_3+\Omega_4+\Theta_3=0$. *Arch. Rat. Mech. Anal.*, to appear
[35] Strang, G. On the Construction and the Comparison of Difference Schemes. *Siam J. Numer. Anal.*, 1968, 5: 506–517
[36] Truesdell, C., Muncaster, R.G. Fundamentals of Maxwell'S Kinetic Theory of a Simple Monatomic Gas. Academic Press, New York, 1980
[37] Whitham, G.B. Linear and Nonlinear Waves. Wiley, New York, 1974
[38] Zhong, X. Development and Computation of Continuum Higher-order Constitutive Relations for High Altitude Hypersonic Flow. Ph.D. Thesis, Stanford University, 1991